

REFERENCES

- Akamatsu, H. and Nagamatsu, K. (1947) A new suggestion for a model representing the structure of carbon black. Journal of Colloid Science, 2, 593-598.
- Ashbee, K.H.G. (1993) Fundamental principles of fiber reinforced composites. 2nd ed. Lancaster: Technomic.
- Baughman, R.H. (1996) Conducting polymer artificial muscles. Synthetic Metals, 78, 339-353.
- Buchko, C.J., Chen, L.C., Shen, Y., and Martin, D.C. (1999) Processing and Microstructural Characterization of Porous Biocompatible Protein Polymer Thin Films. Polymer, 40, 7397-7407.
- Cheng, Z.Y., Bharti, V., Xu, T.B., Xu, H., Mai, T., and Zhang, Q.M. (2001) Electrostrictive poly(vinylidene fluoride-trifluoroethylene) copolymers. Sensor Actuator: A, 90, 138-147.
- Cohen, Y.B. (2001) Electroactive Polymers as Artificial Muscles. Seattle WA: Structures Dynamics and Materials Conference (SDM), Gossamer Spacecraft Forum (GSF), April 16-19.
- Cohen, Y.B., Xue, T., Joffe, B., Lih, S.S., Shahinpoor, M., Simpson, J., Smith, J., and Willis, P. (1997) Enabling Technologies: Smart Structures and Integrated Systems. San Diego: The SPIE International Conference, Smart Structures and Materials Symposium.
- Deitzel, J.M., Kleinmeyer, J.D., Hirvonen, J.K., and Beck, T.N.C. (2001) Controlled deposition of electrospun poly(ethylene oxide) fibers. Polymer, 42, 8163-8170.
- DeMerlis, C.C. and Schoneker, D.R. (2003) Review of the oral toxicity of polyvinyl alcohol (PVA). Food and Chemical Toxicology, 41, 319-326.
- Ding, B., Kim, H.Y., Lee, S.C., Shao, C.L., Lee, D.R., Park, S.J., Kwag, G.B., and Choi, K.J. (2002) Preparation and characterization of a nanoscale poly(vinyl alcohol) fiber aggregate produced by an electrospinning method. Journal of Polymer Science: Part B: Polymer Physics, 40, 1261-1268.
- Doshi, J. and Reneker, D.H. (1995) Electrospinning process and applications of electrospinning. Polymer, 40, 4585-4592.

- Dunn, A.S. (1992) Spectroscopic properties of polyvinyl alcohol. In: Finch CA, editor. Polyvinyl alcohol—developments. Chichester: Wiley.
- Formhals, A. (1934) US Patent No. 1,975,504.
- Frenot, A. and Chronakis I.S. (2003) Polymer nanofibers assembled by electrospinning. Current Opinion in Colloid and Interface Science, 8, 64–75.
- Fulcheri, L., Probst, N., Flamant, G., Fabry, F., Grivei, E., and Bourrat, X. (2002) Plasma processing: a step towards the production of new grades of carbon black. Carbon, 40, 169-176.
- Furukuwa, T. (1997) Structure and functional properties of ferroelectric polymers. Advance Colloid Interface Science, 71-72, 183-208.
- Gibson, P.W., Schreuder-Gibson, H.L., and Rivin, D. (1999) Electrospun fiber mats: Transport properties. American Institute of chemical Engineers, 45(1), 90-195.
- Griffith, A.A. (1921) The phenomena of rupture and flow in solids. Philosophical Transactions Royal Society, 221, 163-198.
- Gordon, J.E. (1988) The new science of strong materials or why you don't fall through the floor. Princeton: Princeton University Press.
- Gouma, P.I. (2003) Nanostructured polymorphic oxides for advanced chemosensors. Review of Advance Materials Science, 5, 147-154.
- Hafemann, B., Ensslen, S., Erdmann, C., Niedballa, R., Zühlke, A., Ghofrani, K., and Kirkpatrick, C.J. (1999) Use of collagen/elastin-membrane for the tissue engineering of dermis. Burns, 25, 373-384.
- Hendricks, C.D., Carson, R.S., Hogan, J.J., and Schneider, J.M. (1964) AIAA J., 2, 4, 733-737.
- Huang, Z.M., Zhang, Y.Z., Kotaki, M., and Ramakrishna, S. (2003) A review on polymer nanofibers by electrospinning and their applications in nanocomposites. Composite Science and Technology, 63, 2223-2253.
- Inganas, O. and Lundstrum, I. (1999) Carbon nanotube muscles. Science, 284, 1281-1282.
- Jäger, K.-M. and McQueen, D.H. (2001) Fractal agglomerates and electrical conductivity in carbon black polymer composites. Polymer, 42, 9575-9581.

- Jun, Z., Hou, H., Wendorff, H.J., Greiner, A. (2005) Poly(vinyl alcohol) nanofibres by electrospinning: influence of molecular weight on fibre shape. e-Polymer, 038, 1-7.
- Kaneto, K., Kaneto, M., Min, Y., and Macdiarmid, A.G. (1995) Artificial muscle: electromechanical actuators using polyaniline films. Synthetic Metals, 71, 2211-2212.
- Kessick, R. and Tepper, G. (2006) Electrospun polymer composite fiber arrays for the detection and identification of volatile organic compounds. Sensors and Actuators B, in press.
- Koshi, A., Yim, K., and Shivkumar, S. (2004) Effect of molecular weight on fibrous PVA produced by electrospinning. Materials Letters, 58, 493-497.
- Kuptsov, A.H. and Zhizhin, G.N. (1998) Handbook of Fourier Transform Raman and Infrared Spectra of Polymers. Amsterdam: Elsevier.
- Lee, H.J., Chin, B.D., Yang, S.M., and Park, O.O. (1998) Surfactant effect on the stability and electrorheological properties of polyaniline particle suspension, Journal of Colloid Interface Science, 206, 424-438.
- Lee, J.S., Choi, K.H., Ghim, H.D., Kim, S.S., Chun, D.H., Kim, H.Y., and Lyoo, W.S. (2004) Role of molecular weight of atactic poly(vinyl alcohol) (PVA) in the structure and properties of PVA nanofabric prepared by electrospinning. Journal of Applied Polymer Science, 93, 1638-1646.
- Lyons, J. and Ko, F.F. (2004) Nanofibers. Encyclopedia of Nanoscience and Nanotechnology. ed. H.S. Nalwa. Vol. 6.: American Scientific Publishers.
- Martien, F.L. (1986) Encyclopedia of polymer science and engineering. New York: Wiley.
- Martin, J.E. and Anderson, R.A. (1999) Electrostriction in field-structured composites: Basis for a fast artificial muscles. Journal of Chemical Physics, 11(9), 4273-4280.
- Otero, T.F., Grande, H., and Rodriguez, J. (1996) Reversible electrochemical reactions in conducting polymers: a molecular approach to artificial muscles. Journal of Physical Organic Chemistry, 9, 381-386.

- Pelrine, R.E., Kornbluh, R.D., and Joseph, J.P. (1998) Electrostriction of polymer dielectrics with compliant electrodes as a means of actuation. Sensor Actuator: A, 64, 77-85.
- Pomchaitaward, C., Manas-Zloczower, I., and Feke, D.L. (2003) Investigation of the dispersion of carbon black agglomerates of various sizes in simple-shear flows. Chemical Engineering Science, 58, 1859-1865.
- Saikrasun, S., Amornsakchai, T., Sirisinha, C., Meesiri, W., and Bualeklimcharoen, S. (1999) Kevlar reinforcement of polyolefin-based thermoplastic lastomer. Polymer, 40, 6437-6442.
- Seymour, R.B. (1993) Reinforced plastics: properties & applications. 2nd ed. USA: ASM international.
- Shahinpoor, M., Cohen, Y.B., Simpson, J.O., and Smith, J. (1998) Ionic polymer-metal composites (IPMCs) as biomimetic sensors, actuators and artificial muscles-a review. Smart Material Structure, 7, R15-R30.
- Skaarup, S., West, K., and Christiansen B.Z. (1996) Electronically conducting polymers as electrodes and actuators. Solid State Ionics: New Developments, 201-213.
- Son, W.K., Youk, J.H., Lee, T.S., and Park, W.H. (2005) Effect of pH on electrospinning of poly(vinyl alcohol) Materials Letters, 59, 1571-1575.
- Sriupayo, J., Supaphol, P., Blackwell, J., and Rujiravanit, J. (2005) Preparation and characterization of alpha-chitin whisker-reinforced poly(vinyl alcohol) nanocomposite films with or without heat treatment. Polymer, 46, 5637-5644.
- Sui, G.X., Yao, G., and Zhou, B. L. (1995) Influence of artificial pre-stressing during the curing of VIRALL on its mechanical properties. Composites Science and Technology, 53, 361-364.
- Taylor, G. (1969) Electrically Driven Jets. Processing Royal Society, A313. London.
- Tsai, P.P., Schreuder-Gibson, H., and Gibson, P. (2002) Different electrostatic methods for making electret filters. Journal of Electrostatics, 54, 333-341.
- Ueda, T., Kasazaki, T., Kunitake, N., Hirai, T., Kyokane, J., and Yoshino, K. (1997) Polyurethane elastomer actuator. Synthetic Metals, 85, 1415-1416.

- Wu, L., Yuan, X., and Sheng, J. (2005) Immobilization of cellulase in nanofibrous PVA membranes by electrospinning. Journal of Membrane Science, 250, 167-173.
- Zhang, C., Yuan, X., Wu, L., Han, Y., and Sheng, J. (2005) Study on morphology of electrospun poly(vinyl alcohol) mats. European Polymer Journal, 41, 423-432.
- Zeng, J., Aliger, A., Czubyko, F., Kissel, T., Wendorff, J.H., Greiner, A. (2004) Poly(vinyl alcohol) nanofibers by electrospinning as a protein delivery system and the retardation of enzyme release by additional polymer coatings. Biomacromolecules, 6, 1484-1488.

APPENDICES

Appendix A Characterization of Carbon Black

Carbon black (CB) was used in this work was supplied form the East Asiatic Public, Thailand. This company guaranteed that the particle sizes of CB were about 29 nm. SEM was used to check the size as well as the morphological appearance. Moreover, TGA also was used to determine the thermal degradation and water absorption of this CB.

A1. Scanning Electron Images of Carbon Black

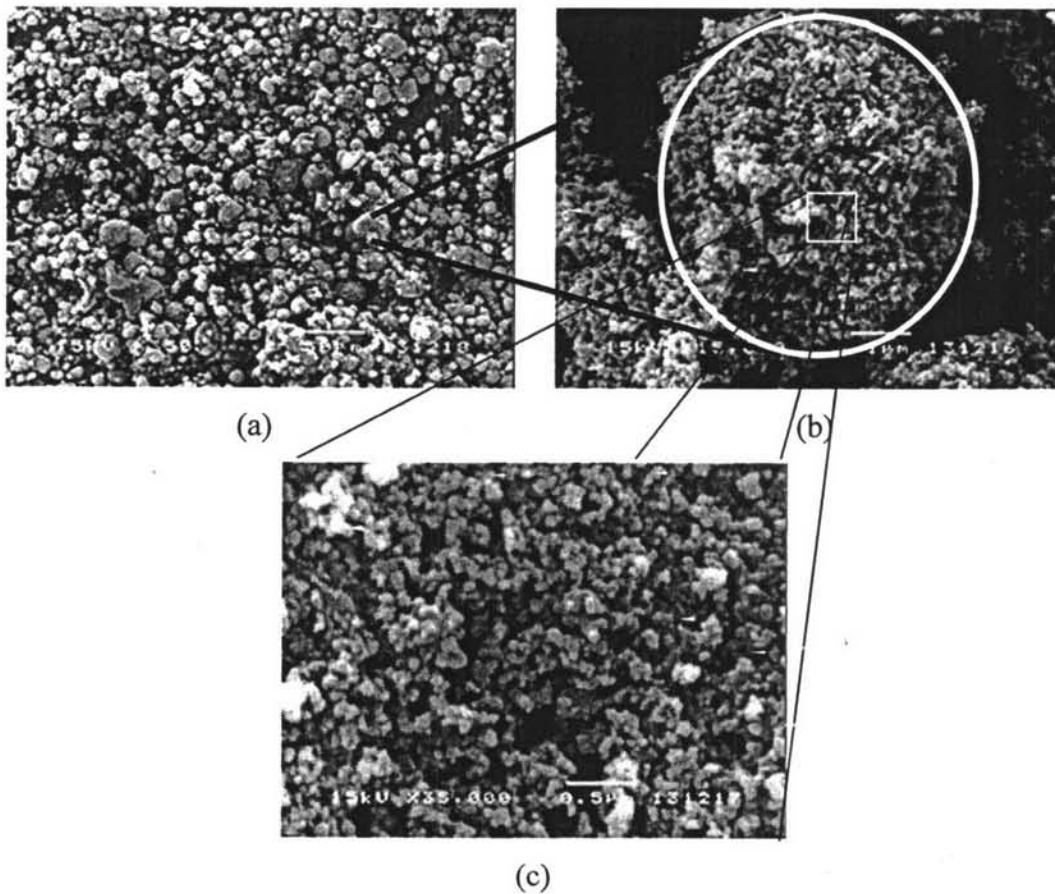


Figure A1 SEM images of Carbon Black; (a) 350x, (b) 15,000x, and (c) 35,000x.

SEM images show that CB was present as individual particles aggregates and agglomerates (see Figure A1). Particles of about 31 ± 0.15 nm and agglomerates of about 8.37 ± 3.16 μm were observed.

A2. Thermogravimetric Thermogram of Carbon Black

The TGA thermogram of CB was observed from a Perkin Elmer Pyris Diamond thermogravimetric-differential thermal analyser (TG-DTA) and showed in Figure A2. The temperature was scanned from 30 to 1,000°C with a heating rate of 10°C/min. The sample was leaved in the ambient weather at 50% relative humidity (RH) for 24 hr, then it was weighted in the range of 5-10 mg and loaded into a platinum pan, finally it was heated under a nitrogen gas flow.

The result illustrated that CB nanoparticles have the moisture contents about 1.64%, and the degradation temperature (onset) of CB is 600 °C and a little bit change at 118 °C.

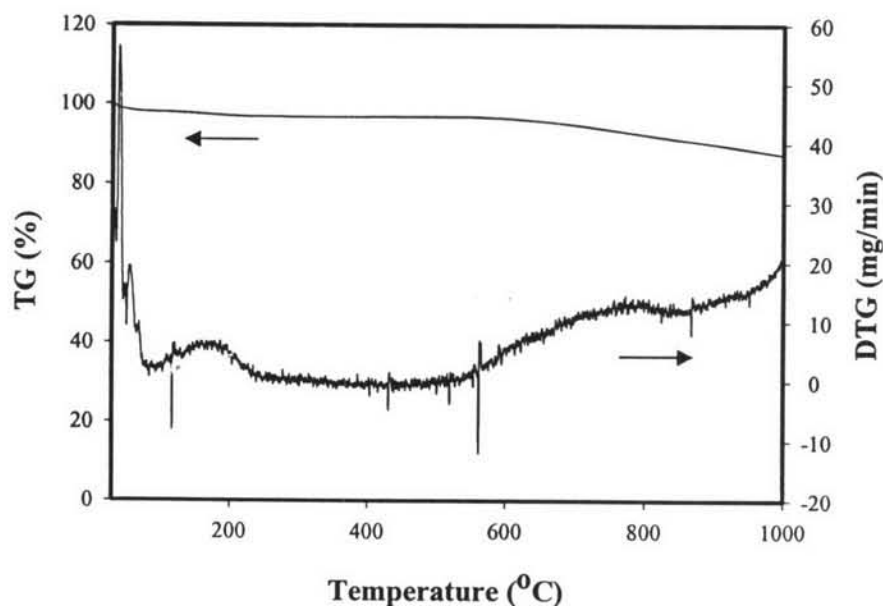


Figure A2 TGA thermogram of carbon black.

Appendix B Carbon Black Dispersion

A JEOL JSM-5200 scanning electron microscope (SEM) was used to investigate the dispersion of CB nanoparticles in 10% (w/v) PVA solution. The 10 wt% CB loading (based on the weight of PVA) was chosen to be the model for study of CB dispersion, because it is the highest CB loading in this work. The correct amount of CB was added to the 40 ml water in a 250-ml round bottom flask. The mixture was sealed tight and sonicated for 8 minutes at 50°C. During this time, the suspension was vigorously shaken (manually) at every 2 hour interval and then stirred for 30 minutes at 85°C. This cycle was repeated 4 times. The required amount of PVA was then added to the mixture and allowed to dissolve with stirring at 85°C for 4 hr. The as-prepared solution was cast to form a thin film prior to characterization by SEM.

The SEM result is shown in Figure B1. It was observed that CB can be dispersed well into individual particles. However, the aggregate formation can still be observed with the size of 101 ± 42 nm. In conclusion, even with the high intensity ultrasonic agitation, complete agglomerate disassociation apparently was not realized. This phenomenon was also reported in many literatures (Jäger *et al.*, 2001; Pomchaitaward *et al.*, 2003).

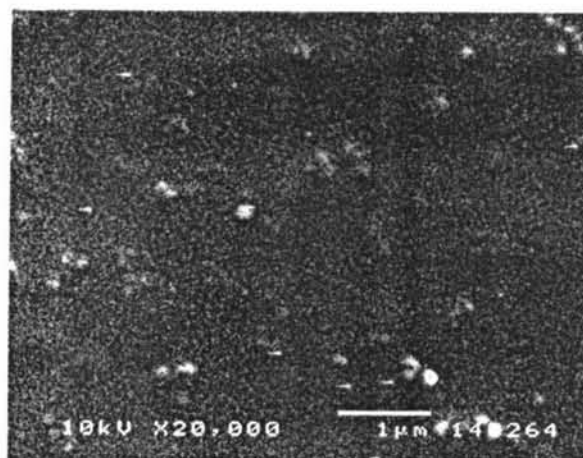


Figure B1 SEM image of 10 wt% CB-loading PVA cast film.

Appendix C Diameter of Deposition Area of Electrospun Fibers

In order to study the effects of solution concentration, applied voltage, collection distance, and CB composition on the deposition diameter of electrospun fibers in electrospinning; the electrospinning experiment with the grounded target plat collector (a sheet of aluminum foil on a plastic backing) was set-up. Optical images of as-spun fibers were taken by a Fujifilm S304 digital camera. The deposition diameters of electrospun fibers in each condition were measured directly from deposited fibers on aluminum foil.

For the study of effects of concentration and applied potential, spinning solutions at various concentrations in the range of 6 to 14% (w/v) were electrospun under various applied potentials in the range of 12.5 to 25 kV over a fixed collection distance of 15 cm. The results are shown in Table C1 and the average deposition diameters of the as-spun fibers are summarized in Table C2.

For the study of effects of collection distance, 10% (w/v) PVA solutions were electrospun under a fixed applied potential of 15 kV over various collection distances in the range of 5 to 20 cm. The results are shown in Table C3 and the average deposition diameters of the as-spun fibers are summarized in Table C4.

For the study of effects of CB composition, 10% (w/v) PVA solutions were electrospun under a fixed applied potential of 15 kV over a fixed collection distances of 15 cm. The collection time was fixed for all conditions at 1 min. The results are shown in Table C5 and the average deposition diameters of the as-spun fibers are summarized in Table C6.

C1. Effects of Solution Concentration and Applied Potential (Fixed distance = 15 cm)

Table C1. Optical images from the study of effects of solution concentration and applied potential

	6% wt/v	8% wt/v	10% wt/v	12% wt/v	14% wt/v
12.5 kV					
15.0 kV					
17.5 kV					
20.0 kV					
22.5 kV					
25.0 kV					

Table C2. Average deposition diameter (cm) of electrospun fibers from the study of effects of solution concentration and applied potential

	6% wt/v	8% wt/v	10% wt/v	12% wt/v	14% wt/v
12.5 kV	22.0	19.5	18.0	12.0	10.0
15.0 kV	20.0	19.0	15.0	7.5	6.5
17.5 kV	19.0	17.5	13.5	7.0	5.0
20.0 kV	17.0	15.0	12.5	6.0	3.2
22.5 kV	15.5	13.5	12.0	4.5	4.5
25.0 kV	13.0	12.5	11.5	4.0	4.5

C2. Effects of Collection Distance (Fixed concentration = 10% w/v, applied voltage = 15 kV)

Table C3. Optical images from the study of effects of collection distance

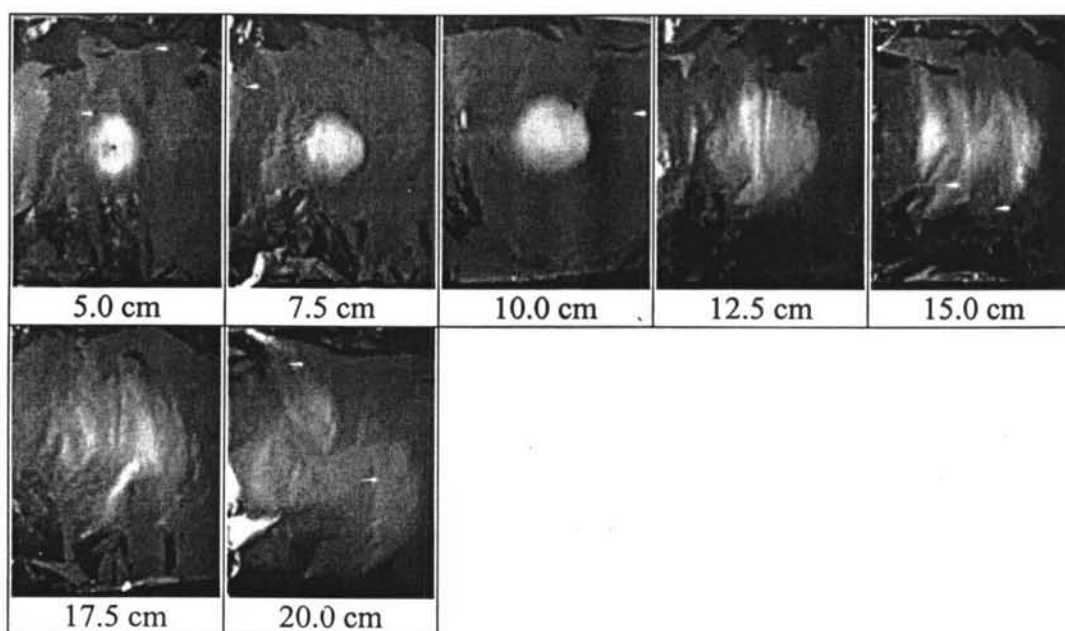


Table C4. Average deposition diameter (cm) of electrospun fibers from the study of collection distance

Deposition diameter (cm)	Collection distance						
	17.5 cm	20.0 cm	5.0 cm	7.5 cm	10.0 cm	12.5 cm	15.0 cm
	3	4.5	6.5	9	12	13.5	17

C3. Effects of CB Composition (Fixed concentration of PVA = 10% w/v, applied voltage = 15 kV, collection distance = 15.0 cm)

Table C5. Optical images from the study of effects of CB composition (wt% is based on weight of PVA)

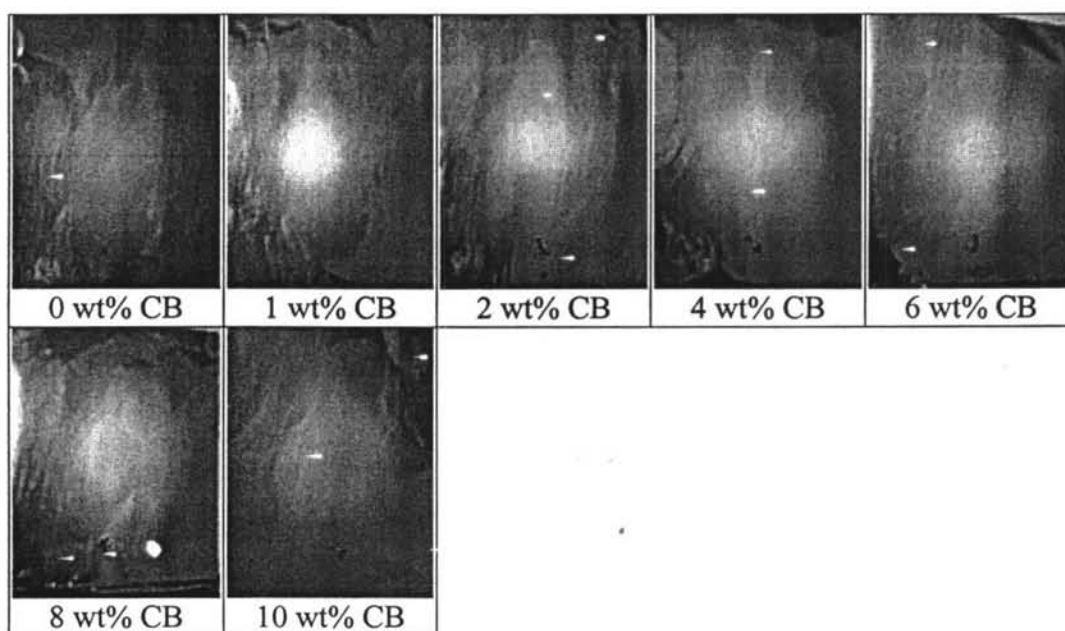


Table C6. Average deposition diameter (cm) of electrospun fibers from the study of CB composition

	0 wt% CB	1 wt% CB	2 wt% CB	4 wt% CB	6 wt% CB	8 wt% CB	10 wt% CB
Deposition diameter (cm)	16	15	14.5	14	14	13.5	12

Appendix D Morphological Appearance and Fiber Diameters

In order to study the effects of solution concentration, applied voltage, collection distance, and CB composition on the morphological appearance and fiber diameters, the electrospinning experiment with the grounded target plat collector (a sheet of aluminum foil on a plastic backing) was set-up. A JEOL JSM-5200 scanning electron microscope (SEM) was used to investigate the morphological appearance and fiber diameters of the as-spun fibers. The scanning electron images were obtained by using an acceleration voltage of 10 kV with a magnification of 200, 7,500 and/or 20,000x. The average fiber diameter of the electrospun fibers was measured by Semafore 4.0 software directly from SEM images at the magnification of 7,500x.

For the study of effects of concentration and applied potential, spinning solutions at various concentrations in the range of 6 to 14% (w/v) were electrospun under various applied potentials in the range of 12.5 to 25 kV over a fixed collection distance of 15 cm. Figures D1-D5 show the SEM images results from this study.

For the study of effects of collection distance, 10% (w/v) PVA solutions were electrospun under a fixed applied potential of 15 kV over various collection distances in the range of 5 to 20 cm. Figure D6 shows the SEM images results from this study.

For the study of effects of distance from the center of deposition area and CB composition, 10% (w/v) PVA solutions were electrospun under a fixed applied potential of 15 kV over a fixed collection distances of 15 cm. The collection time was fixed for all conditions at 1 min. Figures D8 and D9 show the SEM images results from the study of effects of distance from the center of deposition area and CB composition, respectively.

D1. Effects of Solution Concentration and Applied Potential (Fixed collection distance = 15 cm)

D1.1 6% (w/v) PVA

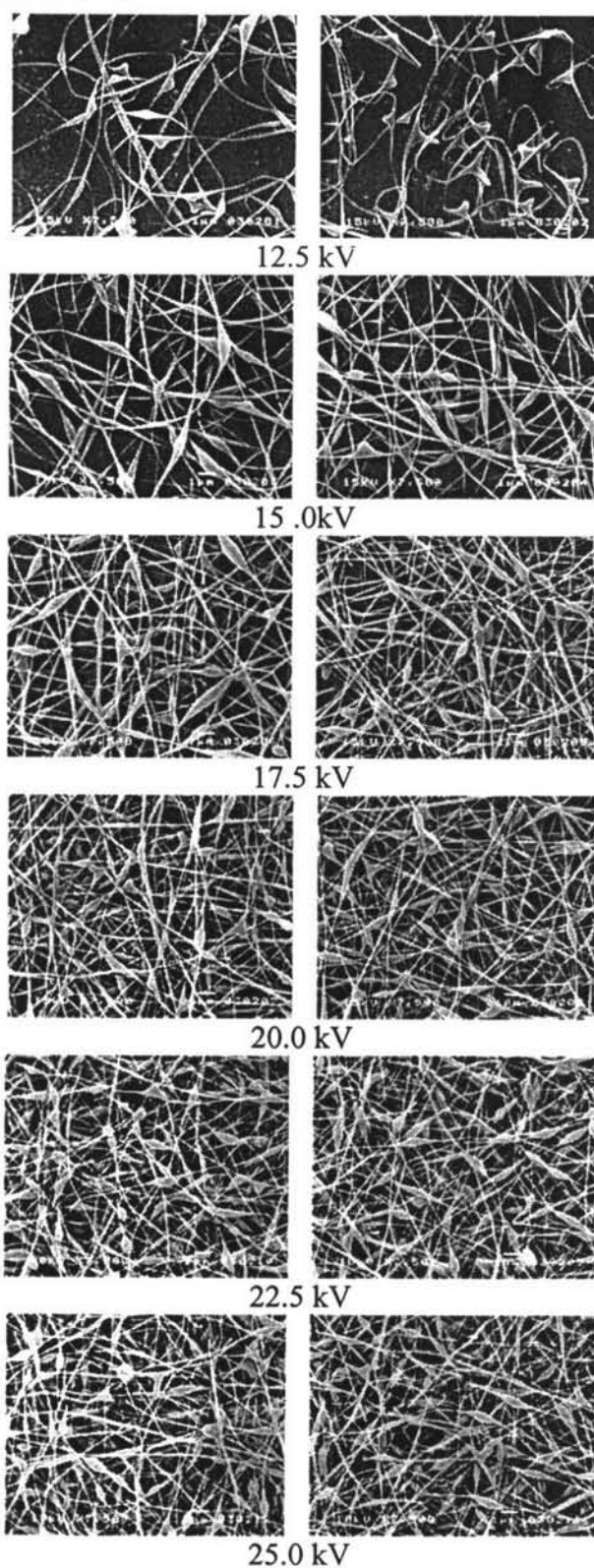


Figure D1 SEM images of as-spun PVA fibers from 6% (w/v) PVA solutions at various applied potentials. The collection distance was fixed at 15 cm.

D1.2 8% (w/v) PVA

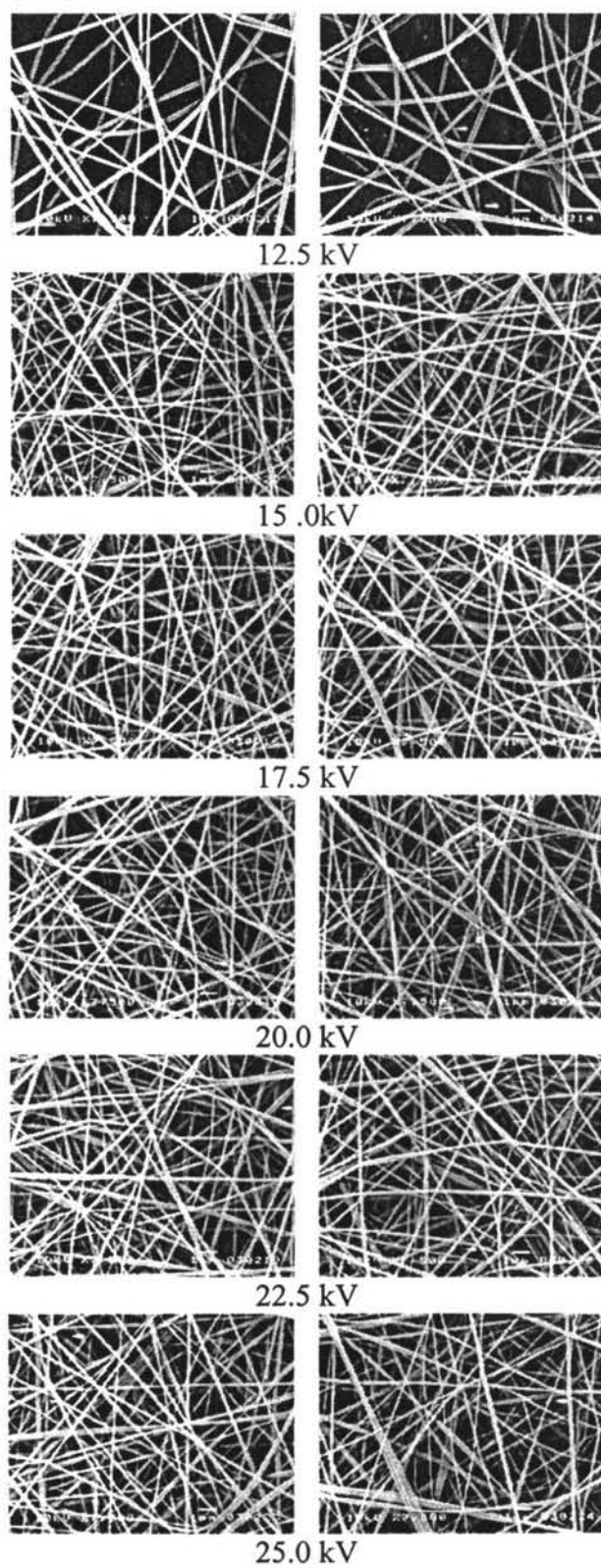


Figure D2 SEM images of as-spun PVA fibers from 8% (w/v) PVA solutions at various applied potentials. The collection distance was fixed at 15 cm.

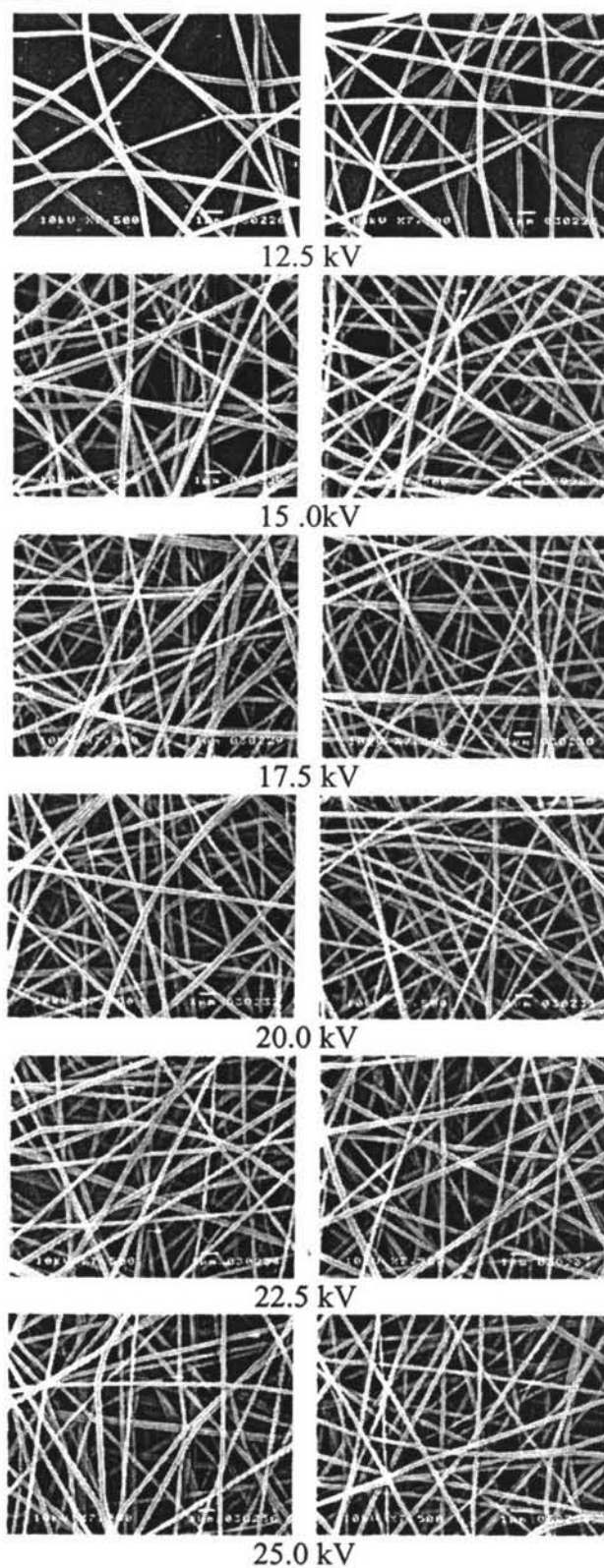
D1.3 10% (w/v) PVA

Figure D3 SEM images of as-spun PVA fibers from 10% (w/v) PVA solutions at various applied potentials. The collection distance was fixed at 15 cm.

D1.4 12% (w/v) PVA

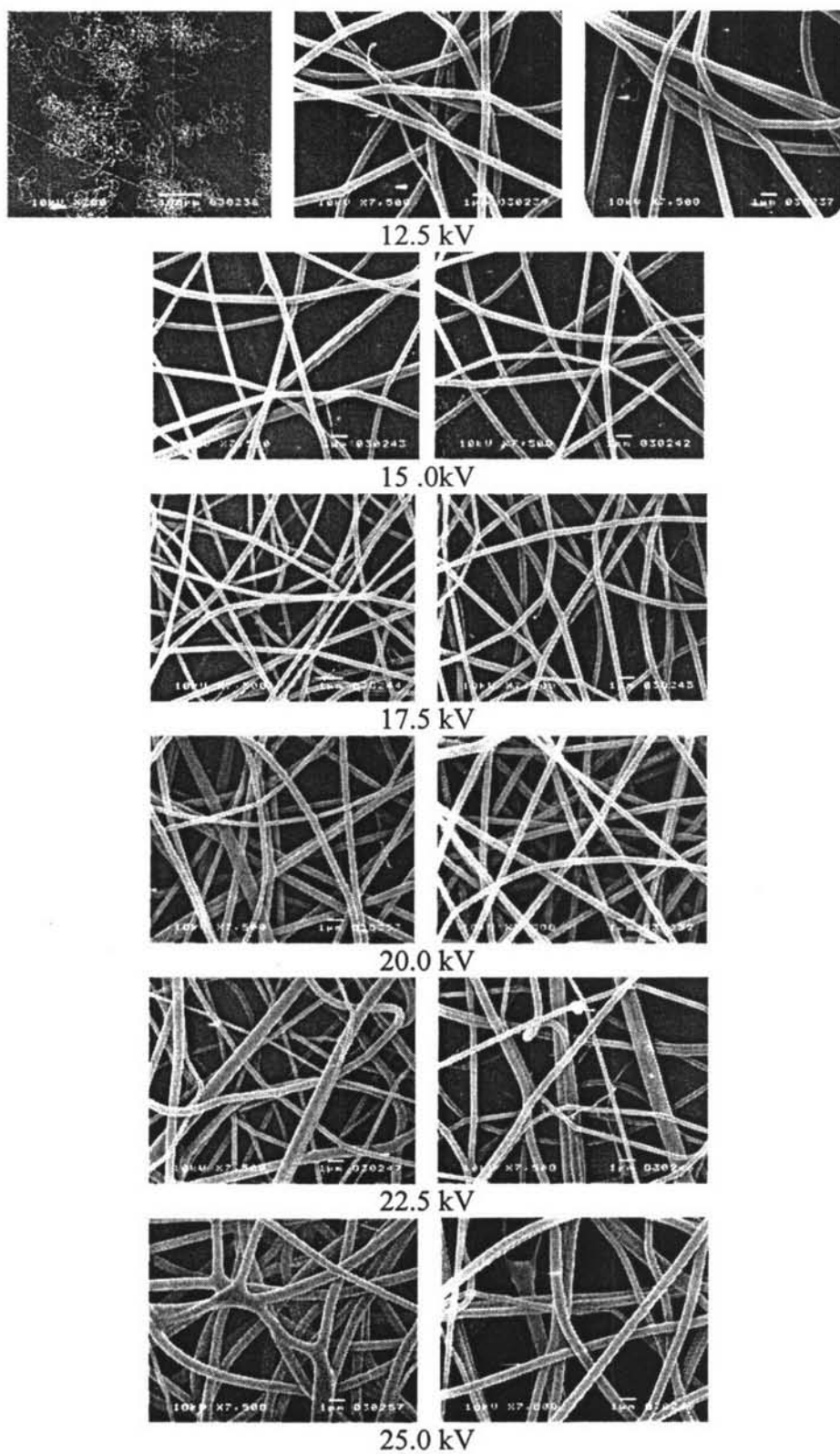


Figure D4 SEM images of as-spun PVA fibers from 12% (w/v) PVA solutions at various applied potentials. The collection distance was fixed at 15 cm.

D1.5 14% (w/v) PVA

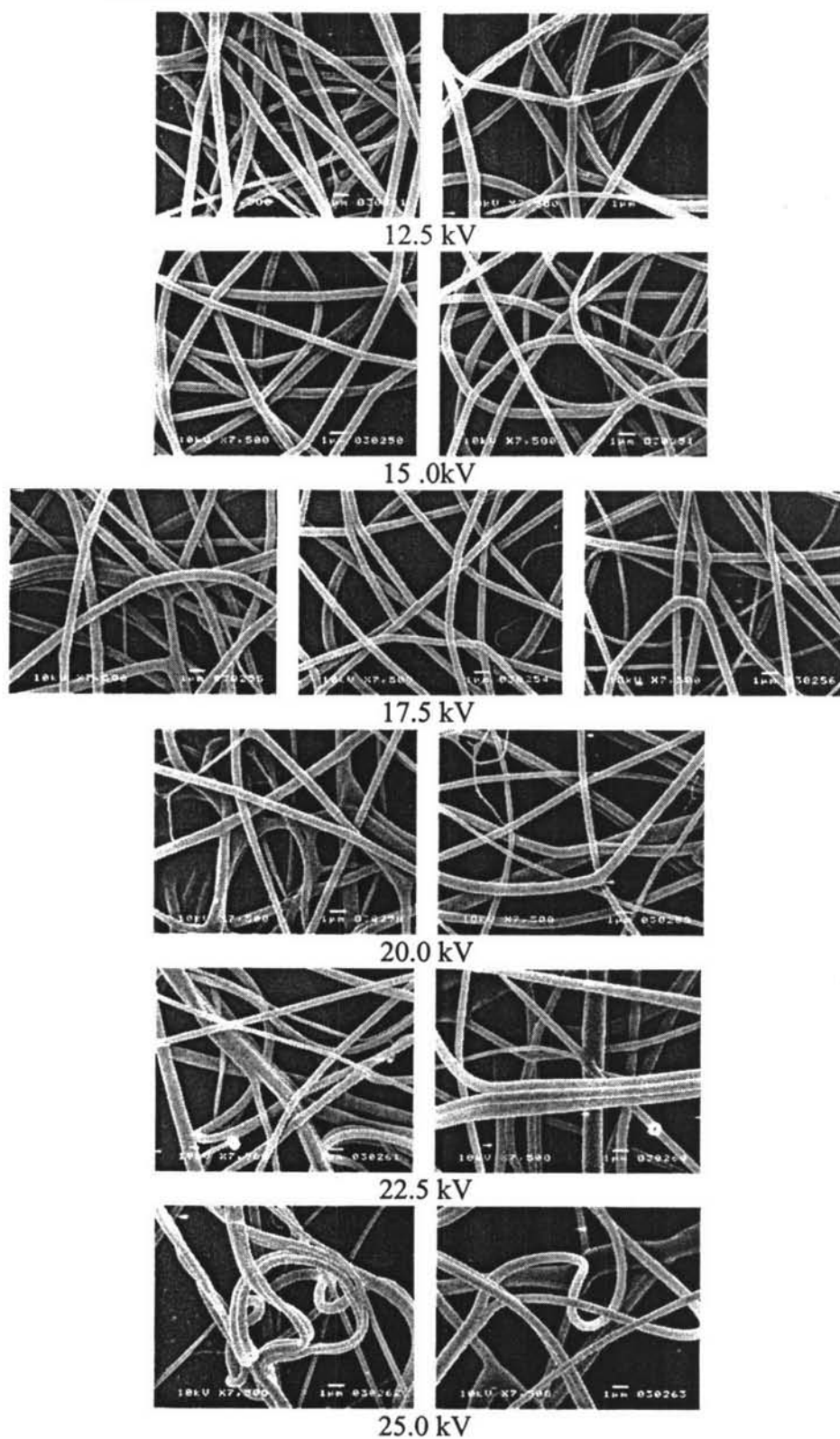


Figure D5 SEM images of as-spun PVA fibers from 14% (w/v) PVA solutions at various applied potentials. The collection distance was fixed at 15 cm.

D2. Effects of Collection Distance (Fixed concentration = 10% w/v, applied potential = 15 kV)

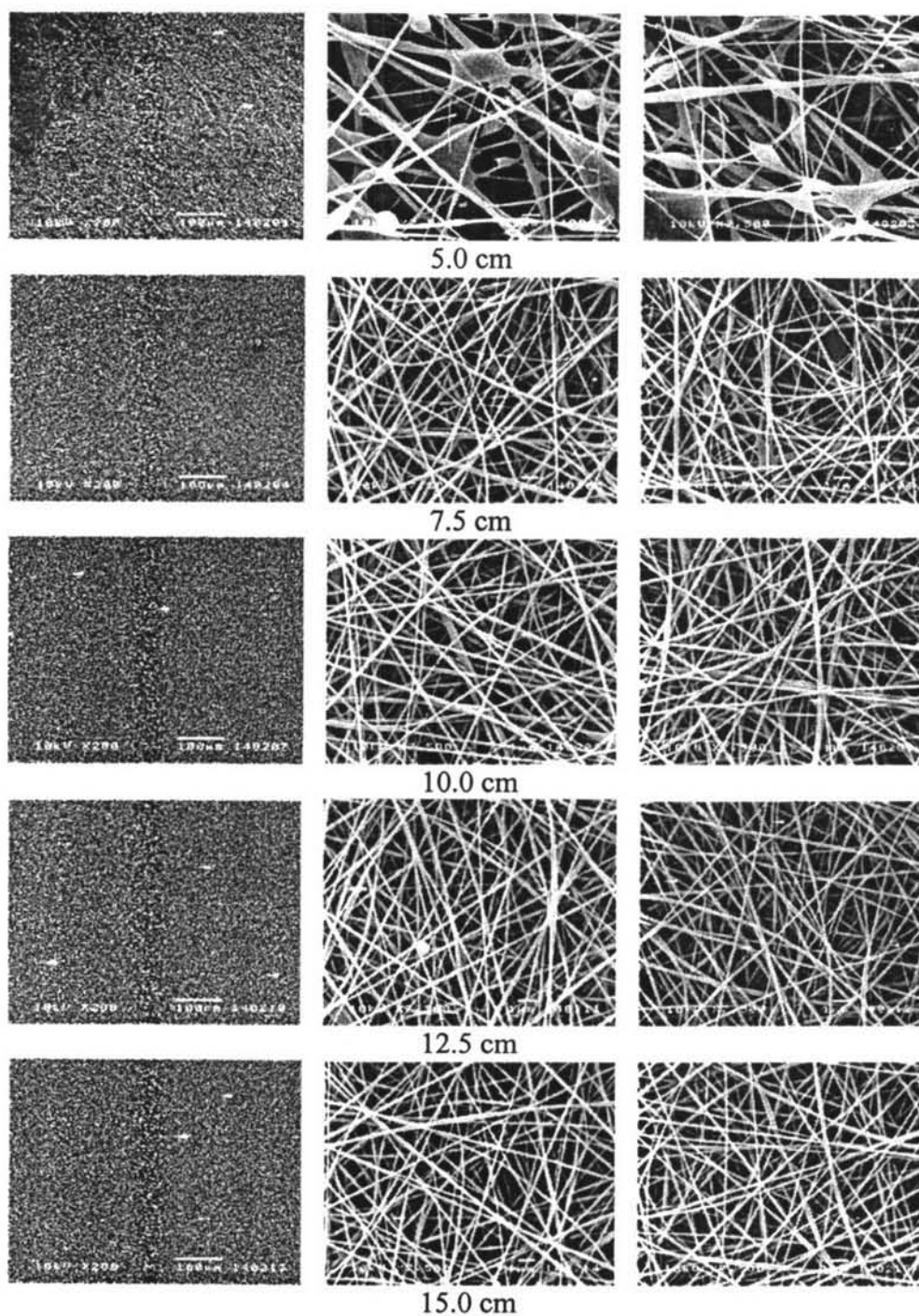


Figure D6 SEM images of as-spun PVA fibers from 10% (w/v) PVA solutions at various collection distances. The applied potential was fixed at 15 kV.

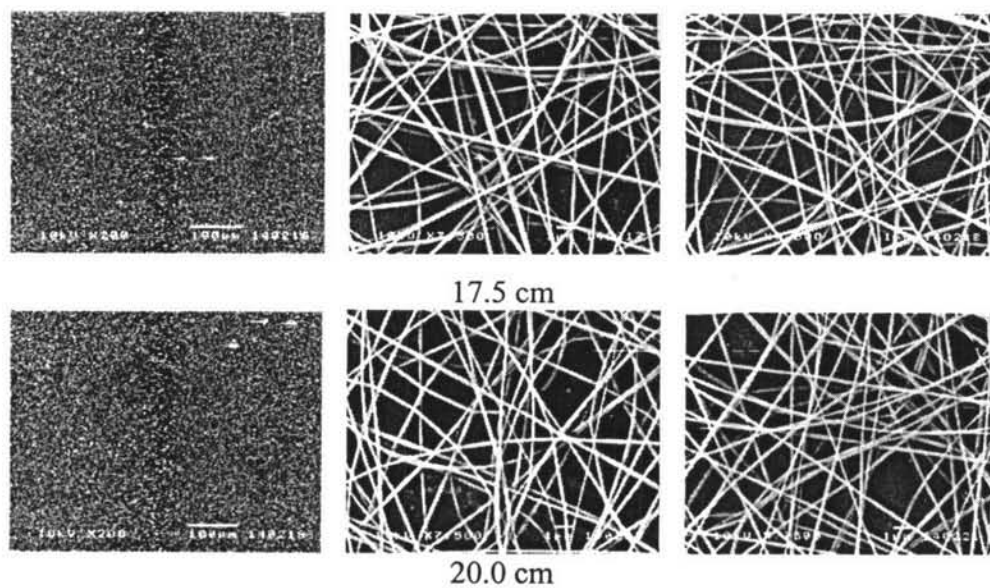


Figure D6 (cont.) SEM images of as-spun PVA fibers from 10% (w/v) PVA solutions at various collection distances. The applied potential was fixed at 15 kV.

D3. Effects of Distance from the Center of Deposition Area (Fixed concentration = 10% w/v, applied potential = 15 kV, collection distance = 15.0 cm)

In order to study the effect of distance from the center of deposition area, the electrospun fibers from 10% PVA (w/v) PVA solutions that were electrospun under applied potential of 15 kV over the collection distance of 15.0 cm were used as the sample. The deposited fiber mats were cut at the positions that far away from the center of deposition area of 0, 3, 6, 9, and 12 cm (see Figure D7). The SEM images results were showed in Figure D8.

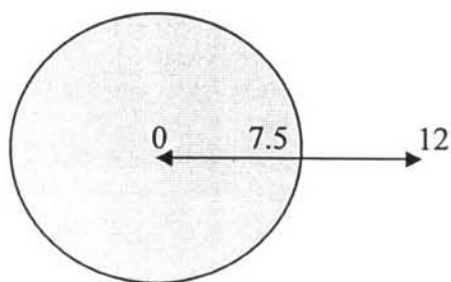


Figure D7 The deposition area (diameter = 15 cm) of electrospun fiber from 10% (w/v) PVA solutions and positions that samples were cut.

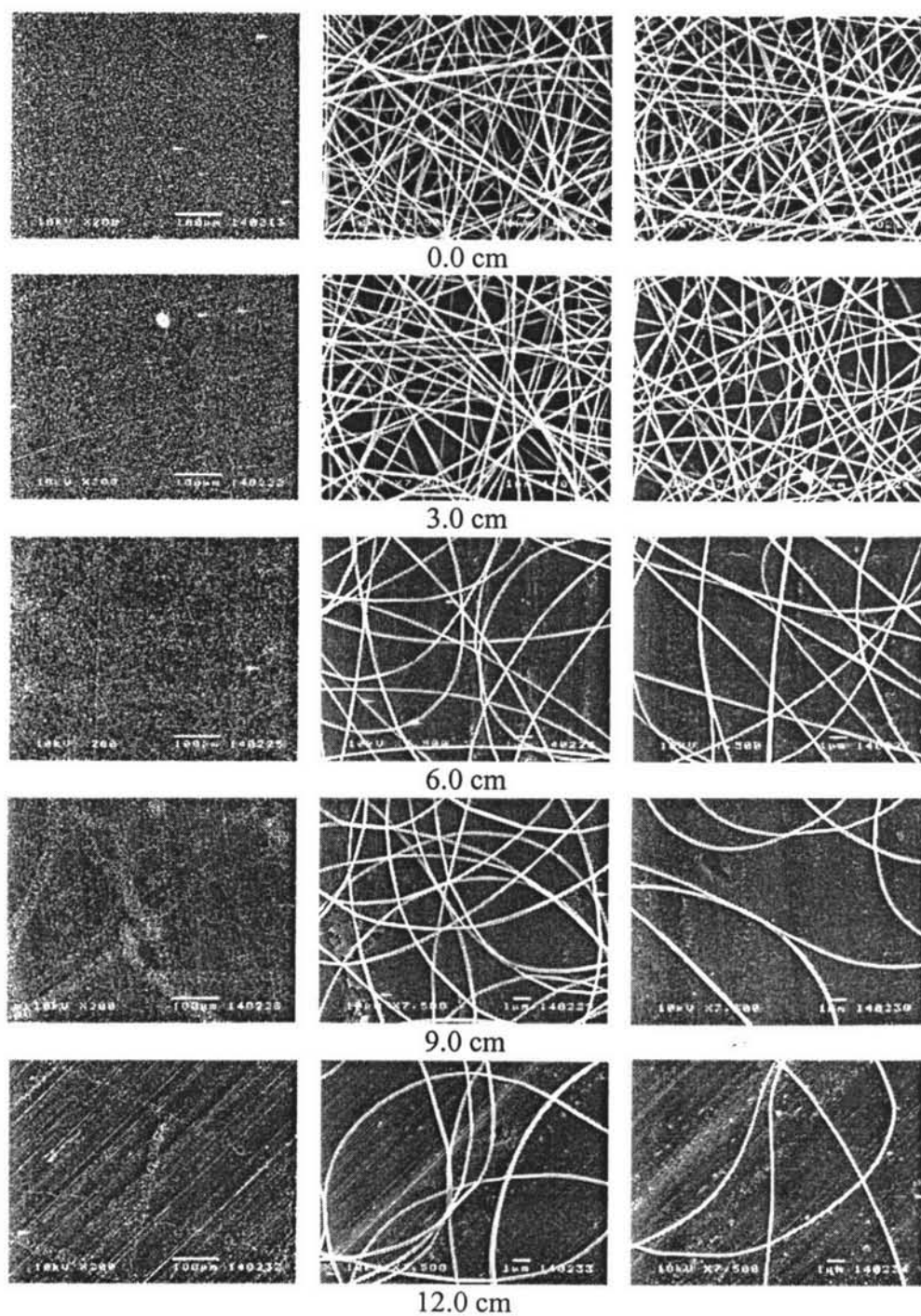


Figure D8 SEM images at various distances from the center (in the range of 0 to 12 cm) of deposition area of the electrospun fibers from 10% PVA (w/v) PVA solutions that were electrospun under applied potential of 15 kV over the collection distance of 15.0 cm.

D4. Effects of CB Composition (Fixed concentration of PVA = 10% w/v, applied voltage = 15 kV, collection distance = 15.0 cm)

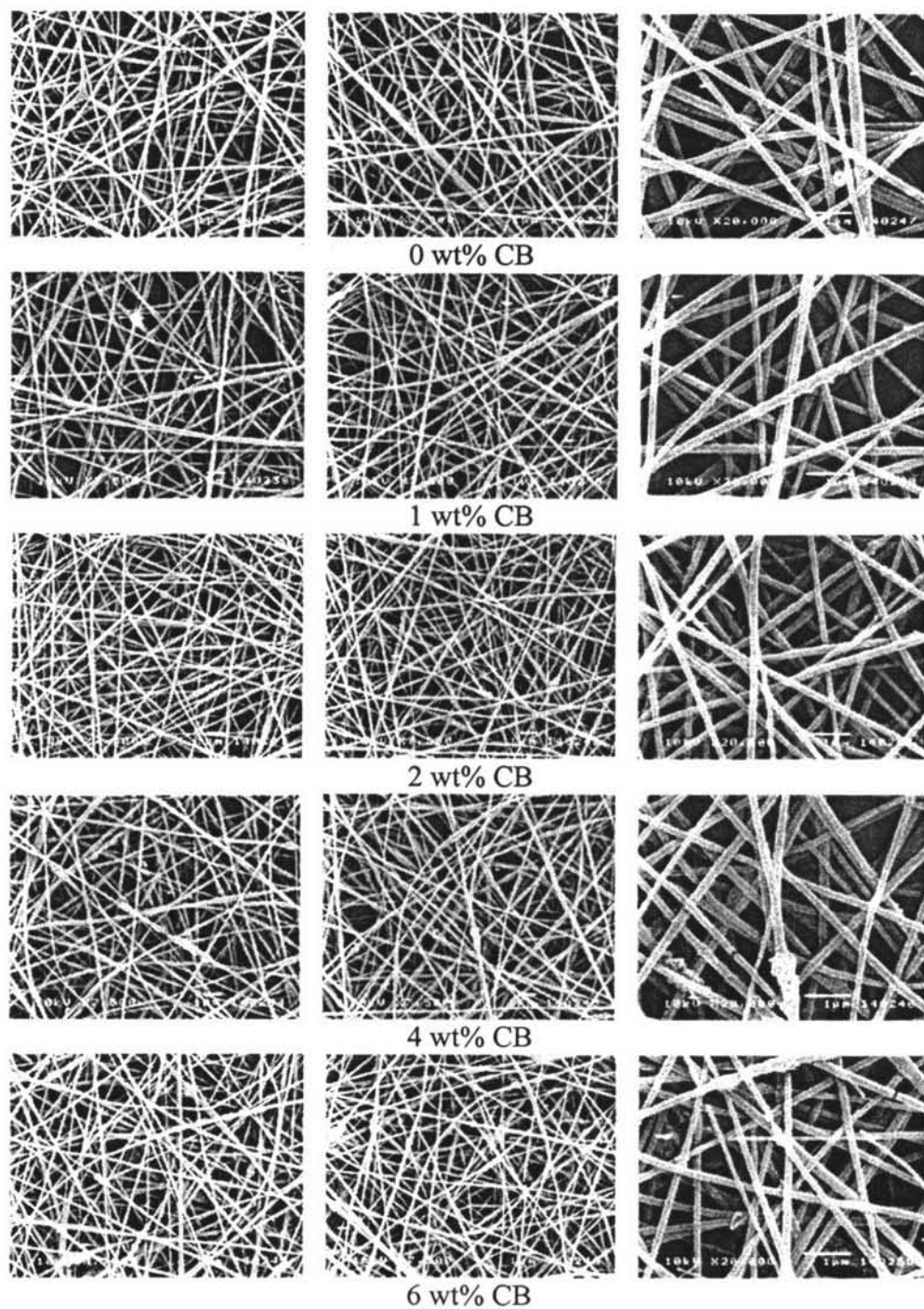


Figure D9 SEM images of as-spun CB-PVA composite fibers from 10% (w/v) PVA solutions at various percentage loadings of CB. The applied potential was fixed at 15 kV over the collection distance 15 cm.

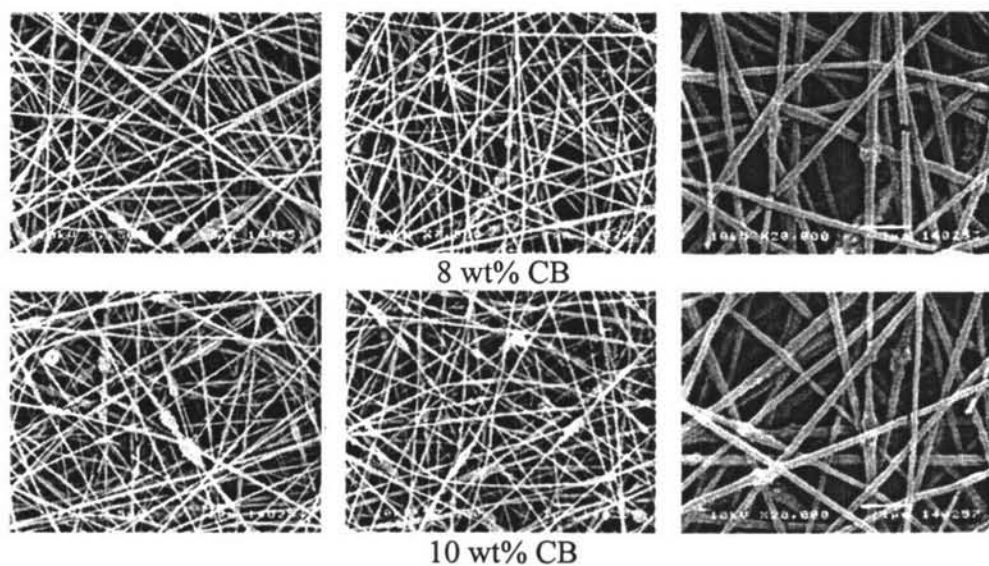


Figure D9 (cont.) SEM images of as-spun CB-PVA composite fibers from 10% (w/v) PVA solutions at various percentage loadings of CB. The applied potential was fixed at 15 kV over the collection distance 15 cm.

Appendix E Viscosity

A Brookfield DV-III programmable viscometer was used to measure the viscosity of the spinning solutions. The measurement was carried out at room temperature ($\sim 27^\circ\text{C}$). The results were reported in both table and figure forms.

E1. Effect of PVA Concentration

Table E1. Viscosity at 27°C of water and as-prepared PVA solutions at various solution concentrations

	PVA solution concentration [% (w/v)]					
	0 (water)	6	8	10	12	14
Viscosity (cP)	1	62	181	810	1932	2430
Speed (rpm)	250	250	250	82.0	25.8	19.9
Shear Rate (sec^{-1})	233	233	233	76.3	24.0	18.5
Torque (%)	0.5	31.0	90.7	100.0	99.8	97.4

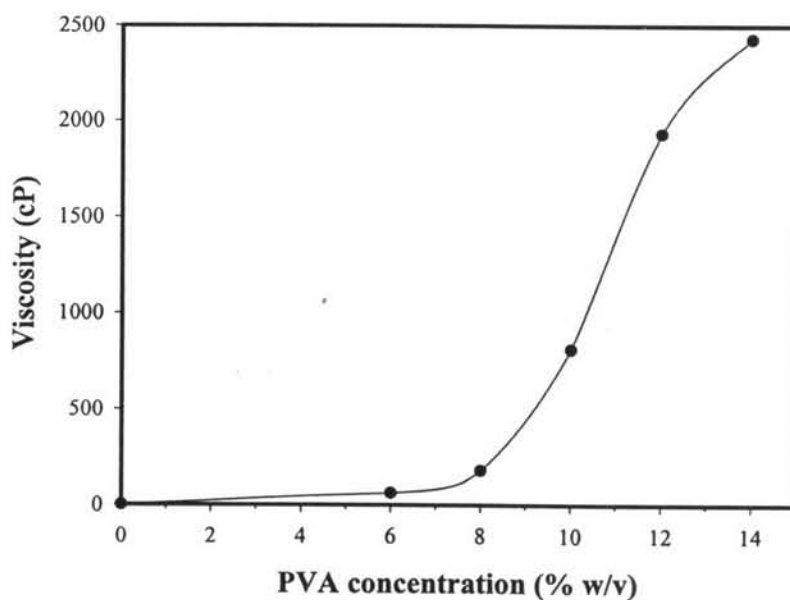


Figure E1. Plot of viscosity as a function of solution concentration for water and as-prepared PVA solutions.

E2. Effect of CB Composition

Table E2. Viscosity of as-prepared PVA and as-prepared CB-loaded PVA solutions at various percentage loadings of CB. The PVA concentration was fixed at 10% (w/v)

	CB composition [wt% CB (base on weight of PVA)]						
	0	1	2	4	6	8	10
Viscosity (cP)	604	601	605	610	655	614	620
Speed (rpm)	82.0	84.0	81.0	81.0	80.0	78.0	76.0
Shear Rate (sec^{-1})	76.3	78.1	75.3	75.3	74.4	72.5	70.7
Torque (%)	99.1	99.7	99.8	99.6	99.4	99.7	99.7

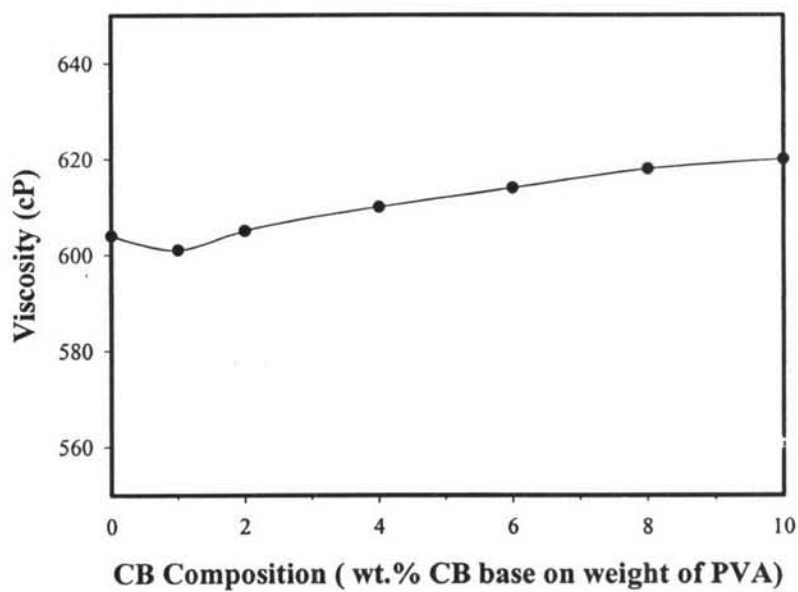


Figure E2. Plot of viscosity as a function of CB composition for as-prepared PVA and as-prepared CB-loaded PVA solutions. The PVA concentration was fixed at 10% (w/v).

Appendix F Conductivity

A Suntex SC 170 conductivity meter was used to measure the viscosity of spinning solutions. The measurement was carried out at the temperature of solution at 25°C. The results were reported in both table and figure forms.

F1. Effect of PVA Concentration

Table F1 Conductivity at 25°C of water and as-prepared PVA solutions at various solution concentrations

	PVA solution concentration [% (w/v)]					
	0 (water)	6	8	10	12	14
Conductivity ($\mu\text{S}/\text{cm}$)	3.88	727	865	1011	1215	1267

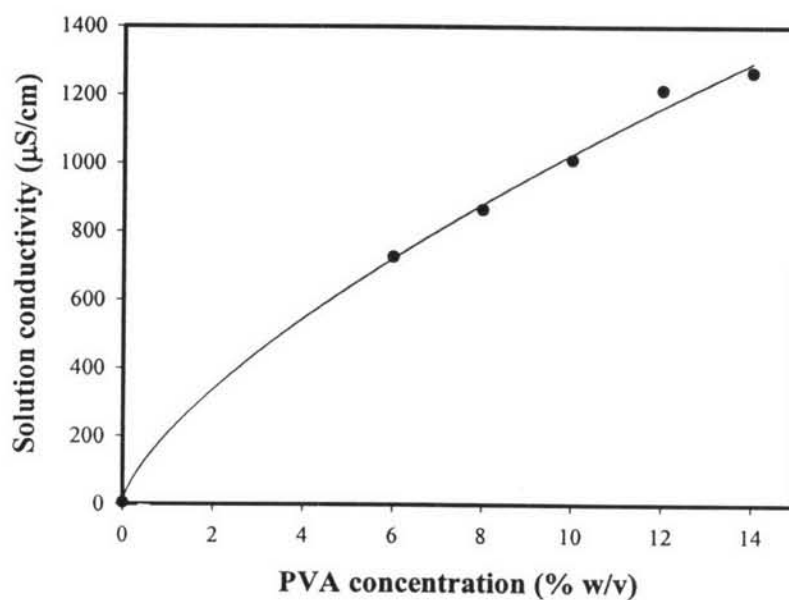


Figure F1 Plot of conductivity as a function of solution concentration for water and as-prepared PVA solutions.

F2. Effect of CB Composition

Table F2 Conductivity of as-prepared PVA and as-prepared CB-loaded PVA solutions at various percentage loadings of CB. The PVA concentration was fixed at 10% (w/v)

	CB composition [wt% CB (base on weight of PVA)]						
	0	1	2	4	6	8	10
Conductivity ($\mu\text{S}/\text{cm}$)	1011	1013	1015	1017	1020	1021	1024

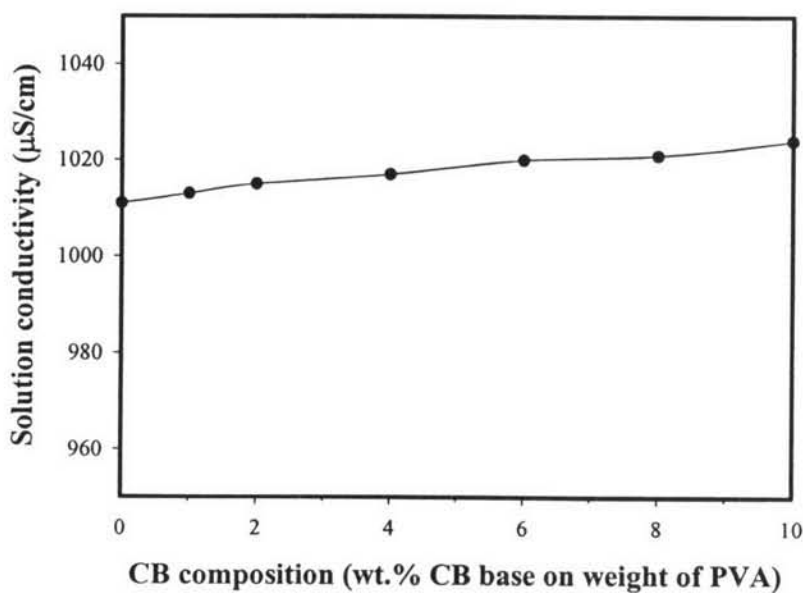


Figure F2 Plot of conductivity as a function of CB composition for as-prepared PVA and as-prepared CB-loaded PVA solutions. The PVA concentration was fixed at 10% (w/v).

Appendix G Color of Electrospun Fibers

A Fujifilm S304 digital camera was used to take an image for illustration of the change in color of as-spun CB-PVA composite fibers with increasing of CB contents (Figure G1).

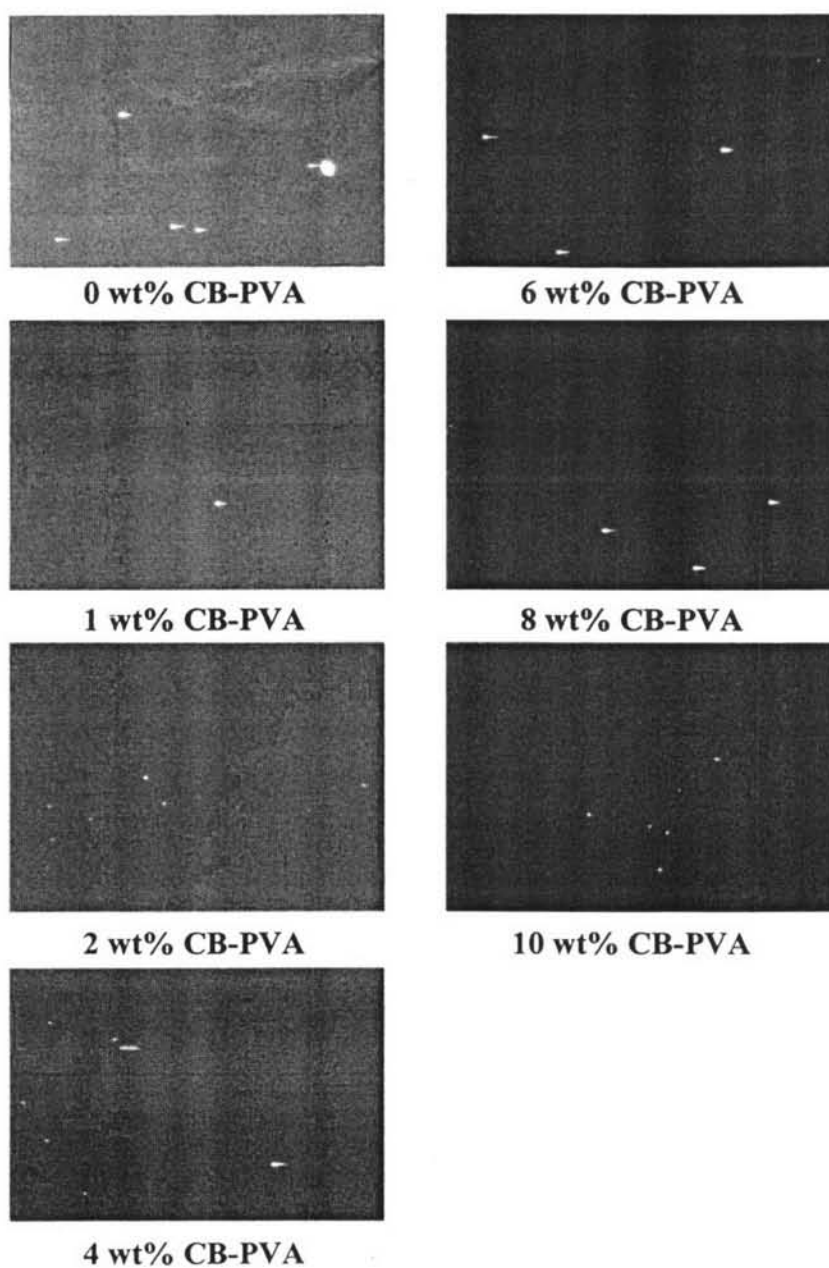


Figure G1 Color of as-spun CB-PVA composite fibers at various CB contents.

Appendix H Fourier-Transformed Infrared Spectroscopy (FT-IR)

A thermo Nicolet Nexus 670 Fourier-transformed infrared spectroscope (FT-IR) was used to identify the functional groups and chemical structure of the as-spun CB-loaded PVA nanofibers, and also used to observe any change in the crystallinity of the as-spun PVA nanofibers.

H1. Effect of thickness of as-spun PVA fiber mat on the IR spectra

Figure H1 shows the IR spectra of as-spun PVA fibers from samples that were tested in direct sample absorption mode with the different thickness. The results show that, in order to obtain the good and smooth peak, the suitable thickness of sample is required.

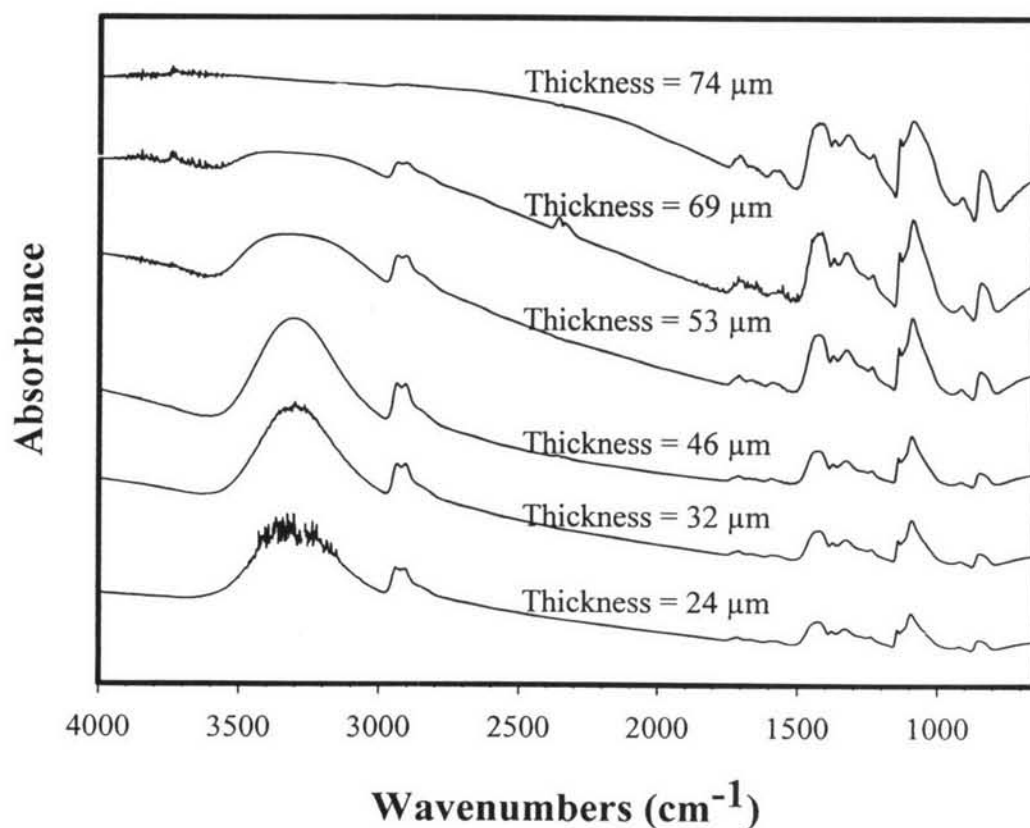


Figure H1 IR spectra of as-spun PVA fibers from samples that were tested in direct sample absorption mode at different thicknesses.

H2. Comparison of direct sample absorption mode and the HATR mode of FT-IR

IR spectra from the studies of effect of CB composition and electric field strength on the structure and crystallinity of PVA electrospun fibers was come from different mode, horizontal attenuated total reflectance (HATR) mode and direct sample absorption mode, respectively. The comparison is required to check the corresponding of these modes. Figure H2 shows this comparison. Apparently, the spectrum form both modes give the peaks at the same positions with the opposite way of relative intensity. This observation refers to the basic of testing modes, reflection and absorption.

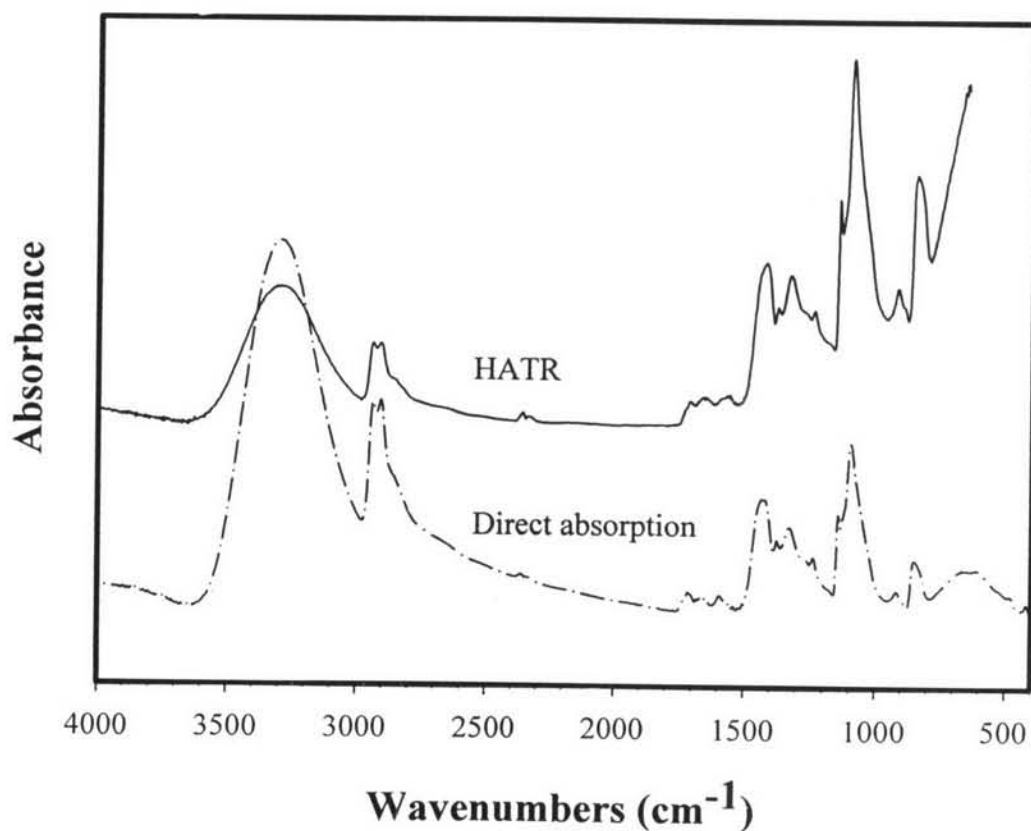


Figure H2. Comparison of IR spectra of as-spun PVA fibers from HATR mode and direct sample absorption mode.

H3. FT-IR of As-Spun PVA Fibers and As-Spun CB Loaded-PVA Fibers

The horizontal attenuated total reflectance (HATR) accessory was used in the characterization of as-spun PVA fibers and as-spun CB loaded-PVA fibers at various CB compositions to investigate some change in chemical structure and crystallinity. The measurements were operated with 32 scans and a resolution of ± 4 cm^{-1} , covering a wavenumber range of $4000\text{-}650$ cm^{-1} . The IR spectra from this study are showed Figure H3.

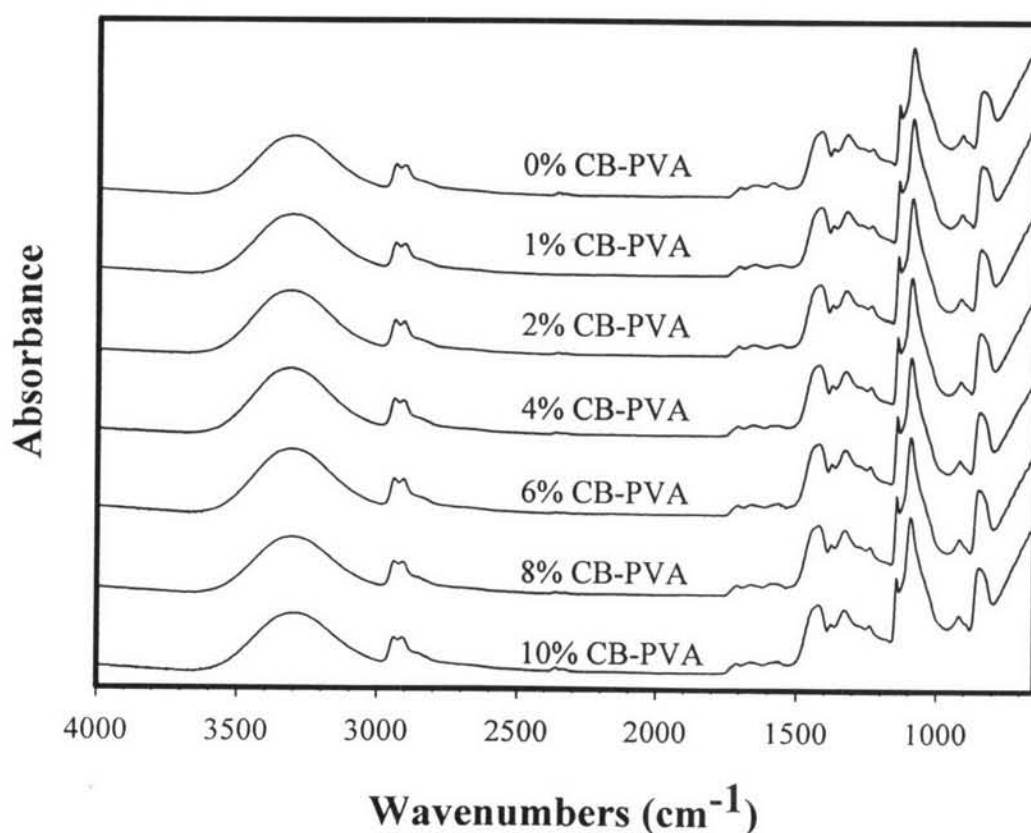


Figure H3. IR spectra of as-spun PVA fibers (0% CB-PVA) and as-spun CB loaded-PVA fibers at various CB compositions.

From Figure H3, IR spectrum of as-spun pure PVA fibers exhibited stretching vibration band of hydrogen-bonded alcohol (-OH) at 3300 cm^{-1} (Kuptsov *et al.*, 1998; Wu *et al.*, 2005). The important point, it was observed that the IR

spectra of as-spun fibers not changed with increasing of percentage contents of CB. It illustrated that no change in structure of PVA with increasing of CB contents. Moreover, it is well known that the adsorption peak at 1144 cm^{-1} [C-O of doubly H-bonded OH in crystalline regions (Dunn, 1992; Sriupayo *et al.*, 2005)] is useful for indication of the crystallinity of PVA. Apparently, the relative intensity of this peak was not found to increase with increasing CB content, indicating that incorporation of CB did not have any effect on the crystallinity of the PVA matrix.

H4. FT-IR of as-Spun PVA Fibers under Various Applied Electrostatic Field

Direct sample absorption mode of FT-IR was use in the characterization of as-spun PVA fibers to investigate the effects of electric field strength on chemical structure and crystallinity of as-spun fibers. The measurements were operated with 32 scans and a resolution of $\pm 4\text{ cm}^{-1}$, covering a wavenumber range of $4000\text{-}400\text{ cm}^{-1}$ using a deuterated triglycine sulfate detector. Figure F4 shows the results from this study.

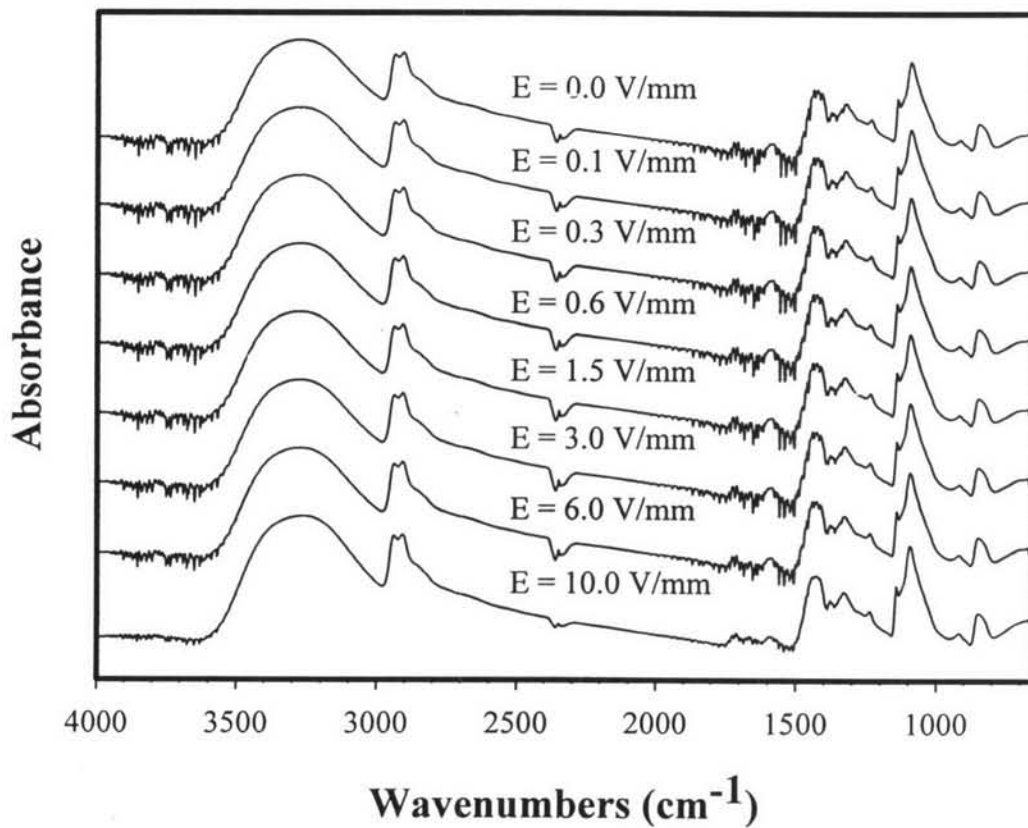


Figure H4. IR spectra of as-spun PVA fibers that were recorded under various electric fields.

IR spectrum of as-spun PVA fibers under all electric fields exhibited absorption peaks at 3300 and 1144 cm^{-1} . Apparently, the relative intensity of this peak was not found to change with variation in the electric field.

Appendix I Wide-Angle X-Ray Diffraction (WAXD)

The measurement of the crystallinity was carried out at room temperature with a Rigaku X-ray diffractometer, connected to a computer. For as-spun fiber mats, 4 layers of each sample were cut into a rectangular shape (2 cm x 2 cm) and laid on the rectangular (1.5 cm x 1.5 cm)-holed metal sample holder. For CB nanoparticles and PVA powder, the samples were packed and smoothly swept off in the window of glass sample holder. The diffraction scans were collected at $2\theta = 3-50^\circ$. The WAXD patterns were showed in Figure I1.

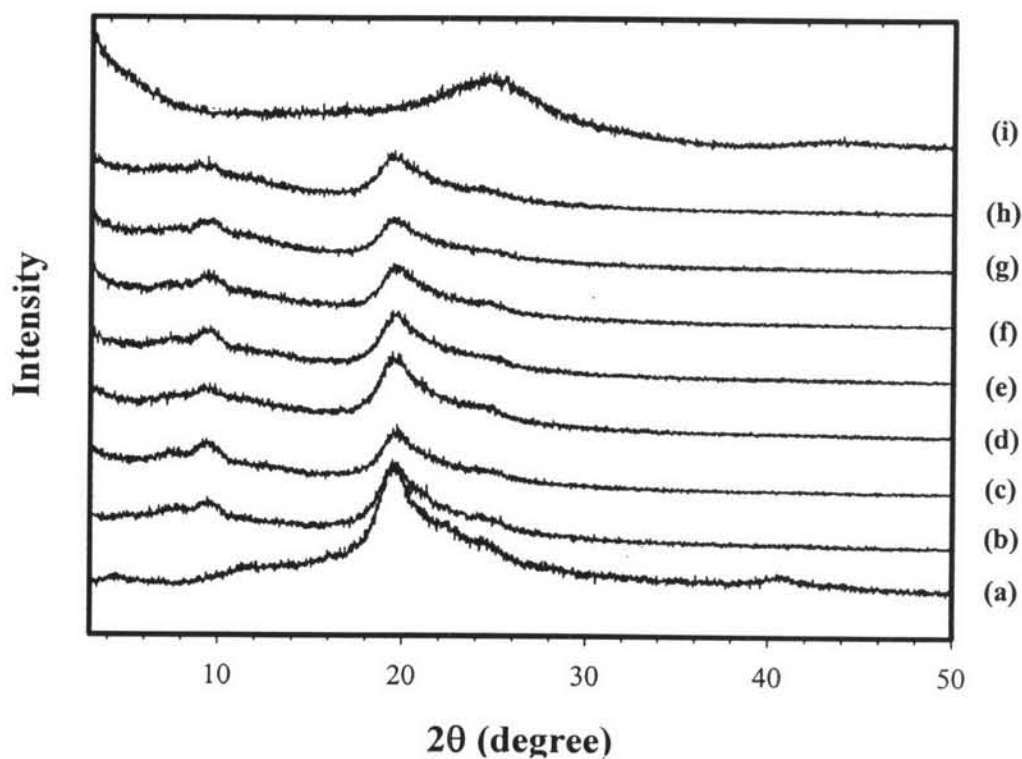


Figure I1 WAXD patterns of: (a) PVA powder; (b) as-spun PVA fibers; (c-h) 1, 2, 4, 6, 8, 10 wt% CB loaded (base on weight of PVA) electrospun PVA fibers, respectively; and (i) CB nanoparticles.

The crystalline properties of electrospinning fibers may be of primary importance when electroactive applications were considered. Figure I1 shows

WAXD patterns of PVA powder, as-spun PVA fibers, as-spun CB-PVA composite fibers, and CB nanoparticles. The reflections of the CB pattern [Figure 11(i)] were broad due to CB is the amorphous carbon (Akamatu *et al.*, 1947). Compared with those of the PVA powder [Figure 11(a)], the peak appeared at the same position ($2\theta \approx 20^\circ$) while the reflections of the as-spun PVA fiber pattern [Figure 11(b)] were relatively broad and strong. Meanwhile, the WAXD pattern of the PVA powder also contained numerous higher order reflections that could not be seen in the fiber pattern (Ding *et al.*, 2002; Lee *et al.*, 2004). The broad and strong nature of the PVA fiber pattern reflections indicated that the crystalline microstructure in the electrospun fibers was significantly greater than that in the PVA powder.

Apparently, the relative intensity and position of the peak of pattern was not found to change with increasing CB content [Figure 11(c-h)], indicating that incorporation of CB did not have any effect on the crystallinity of the PVA matrix. This result is corresponding to FT-IR result.

Appendix J Thermogravimetric Analysis (TGA)

A Perkin Elmer Pyris Diamond thermogravimetric-differential thermal analyser (TG-DTA) was used to determine amount of moisture content and decomposition temperature of CB, PVA powder, and as-spun fibers with the temperature scan from 30 to 1,000°C and a heating rate of 10°C/min. The samples were weighed in the range of 5-10 mg and loaded into a platinum pan, and then they were heated under a nitrogen gas flow. Figures J1 and J2 show the results from this study.

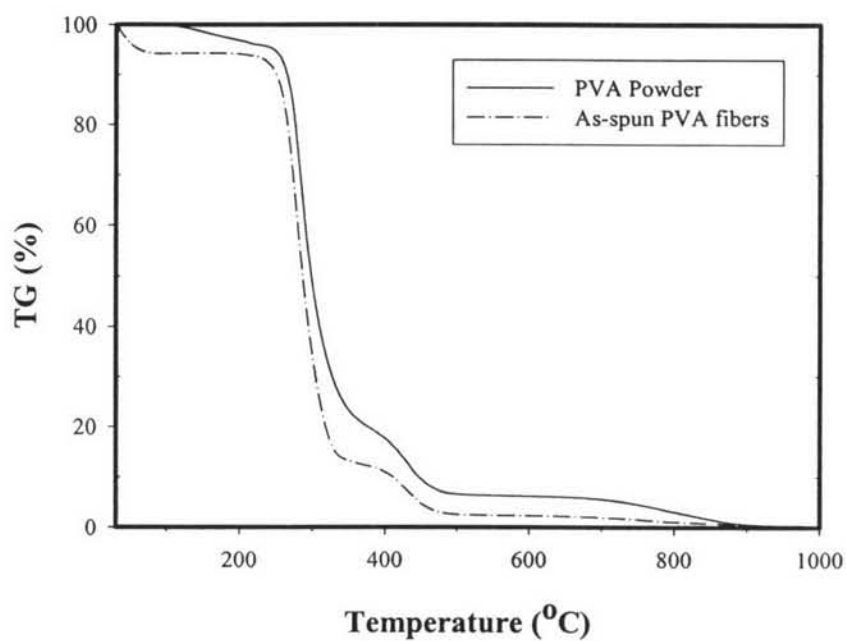


Figure J1 TGA thermogram of PVA powder and as-spun PVA fibers.

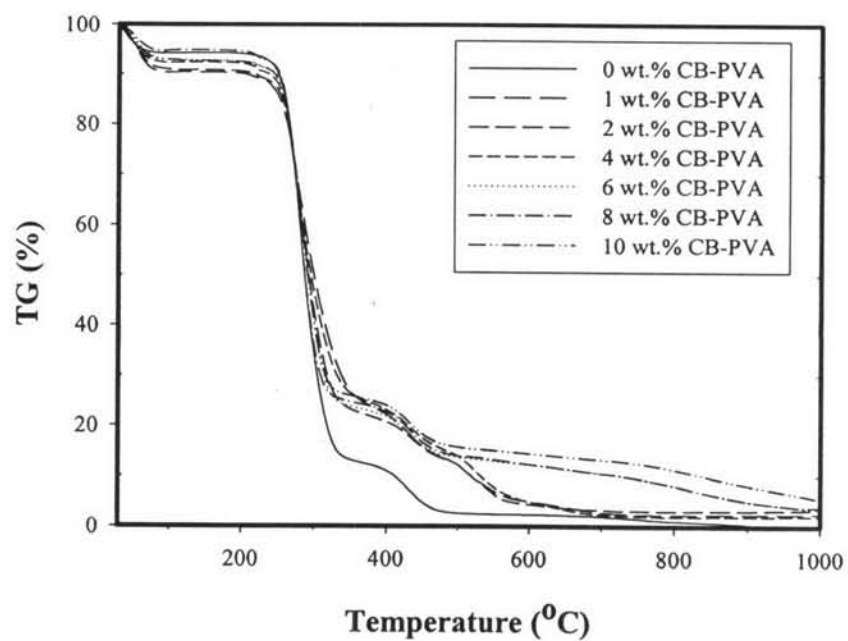
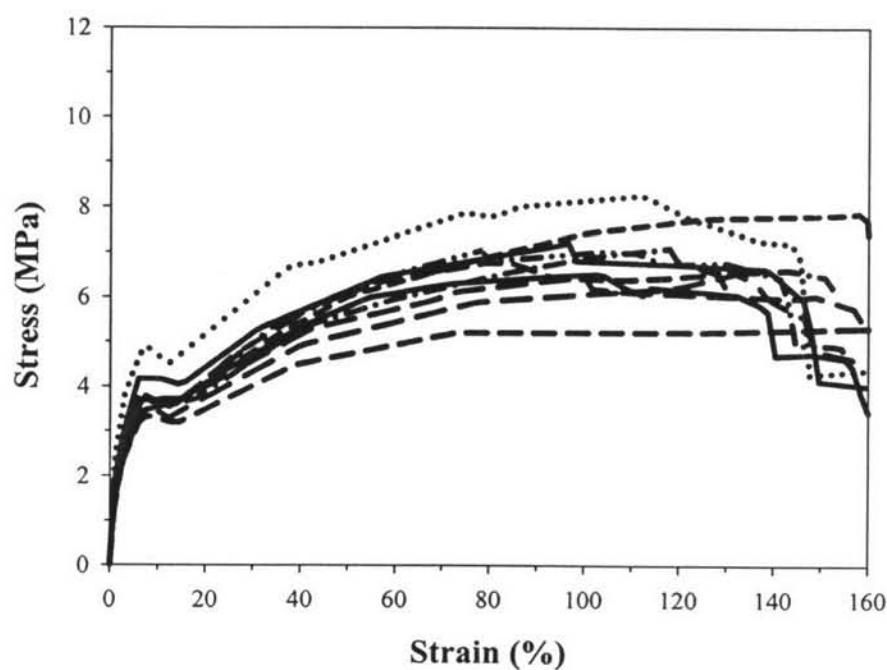


Figure J2 TGA thermogram of as-spun PVA fibers and as-spun CB-loaded PVA fibers at various contents of CB.

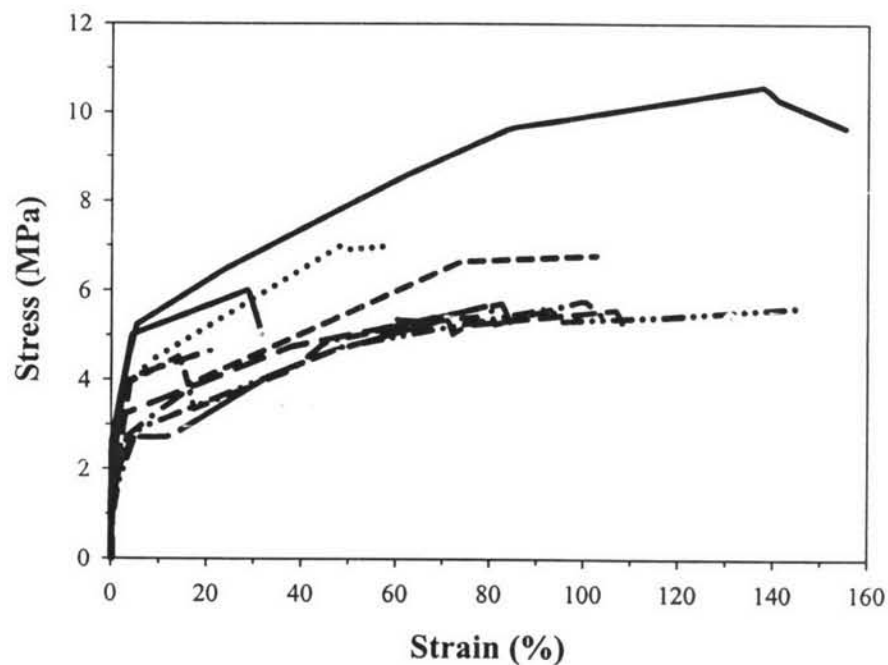
Appendix K Tensile Properties

A Lloyd LRX universal tester was used to investigate the tensile properties of CB filled electrospun nanofiber. The gauge length was 50 mm and the extension rate was 20 mm min^{-1} . As as-spun PVA and composite fibers mats were cut into a rectangular shape ($6 \text{ mm} \times 70 \text{ mm}$) before test.

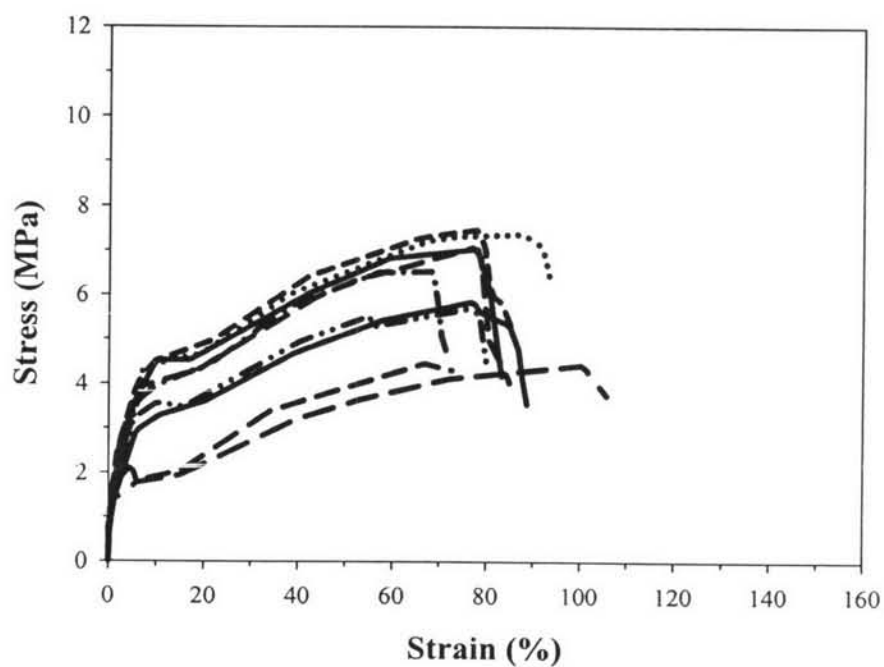
Figures K1-K8 shows the stress-strain curves of pure PVA fibers and 1, 2, 4, 6, 8, and 10% (base on weight of PVA) CB loaded PVA electrospun nanofibers. In addition, the summary of analyzed results of tensile properties was shown in Table K1.



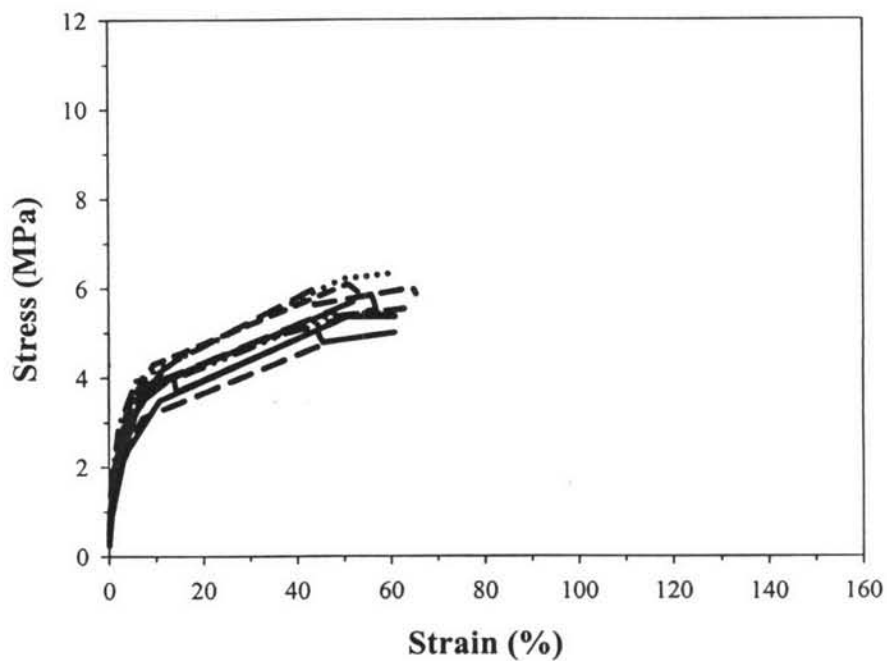
Figures K1 Stress-strain curves of pure PVA fibers from the measurements of 10 specimens.



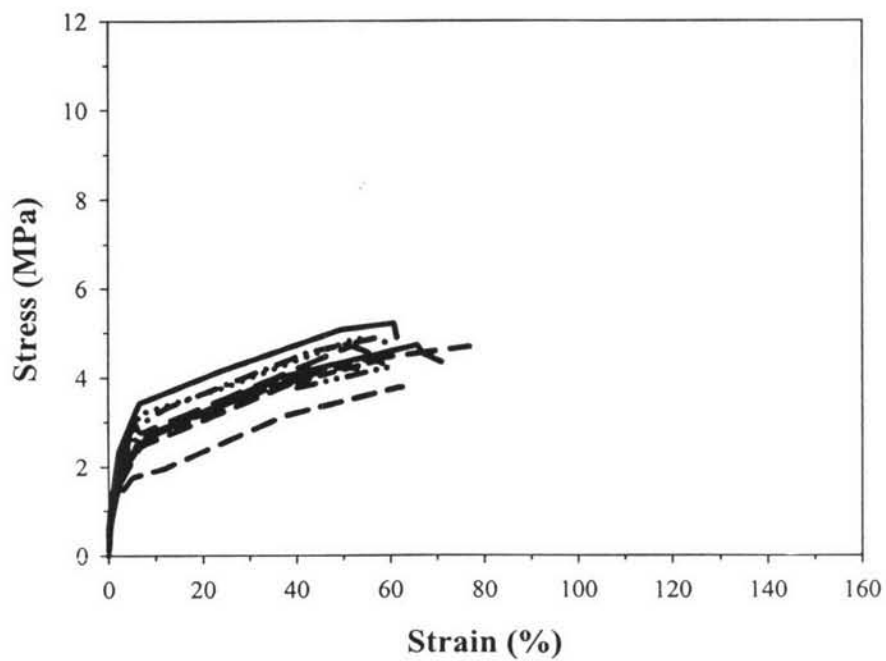
Figures K2 Stress-strain curves of 1 wt% CB-loaded electrospun PVA fibers from the measurements of 10 specimens.



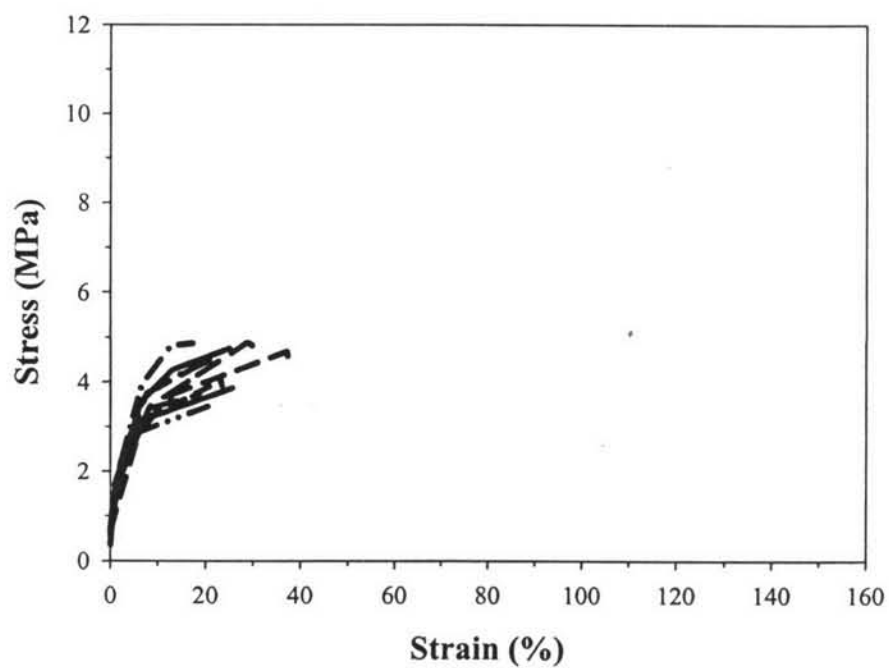
Figures K3 Stress-strain curves of 2 wt% CB-loaded electrospun PVA fibers from the measurements of 10 specimens.



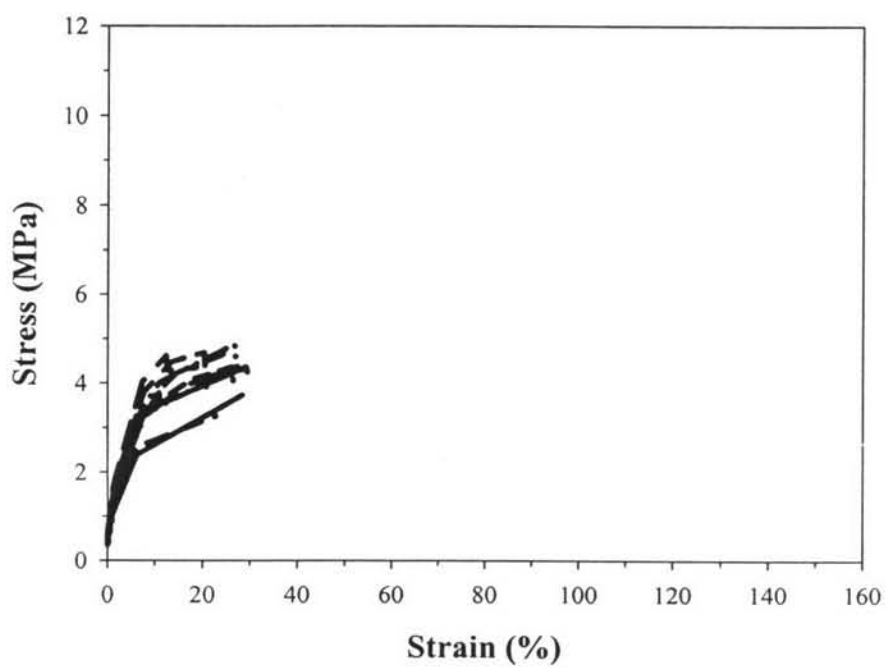
Figures K4 Stress-strain curves of 4 wt% CB-loaded electrospun PVA fibers from the measurements of 10 specimens.



Figures K5 Stress-strain curves of 6 wt% CB-loaded electrospun PVA fibers from the measurements of 10 specimens.



Figures K6 Stress-strain curves of 8 wt% CB-loaded electrospun PVA fibers from the measurements of 10 specimens.



Figures K8 Stress-strain curves of 10 wt% CB-loaded electrospun PVA fibers from the measurements of 10 specimens.

Table K1 Analytical results from tensile properties testing of PVA and CB-loaded PVA electrospun nanofibers

CB contents (wt%) (base on the weight of PVA)	Elastic modulus (Mpa)	Maximum stress (Mpa)	Strain at break (%)
0	80.6 ± 27.2	7.37 ± 2.7	162.2 ± 37.4
1	85.4 ± 13.1	6.29 ± 3.9	115.7 ± 32.8
2	96.3 ± 10.4	6.98 ± 3.4	84.3 ± 11.1
4	127.8 ± 27.5	5.54 ± 2.1	58.8 ± 15.3
6	157.1 ± 10.1	4.56 ± 2.2	58.7 ± 13.7
8	162.5 ± 27.6	4.49 ± 3.5	27.1 ± 5.9
10	155.6 ± 29.8	4.44 ± 1.4	22.9 ± 9.8

Appendix L Electrorheological Properties

A Rheometric Scientific ARES melt rheometer (Figure 3.8a) with a thin fiber/film fixture was used to measure rheological properties of as-spun PVA and CB-loaded PVA fibers. The measurements were carried out under dynamic tension mode and applied electric field strength varying from 0 to 130 V/mm. In these experiments, the dynamic moduli (G' and G'') were measured as functions of frequency and electric field strength. Strain sweep tests were first carried out to determine the suitable strain to measure G' and G'' in the linear viscoelastic regime following by frequency sweep test with the fixed strain in linear viscoelastic regime. The results show in following figures.

L1. 0% CB-PVA

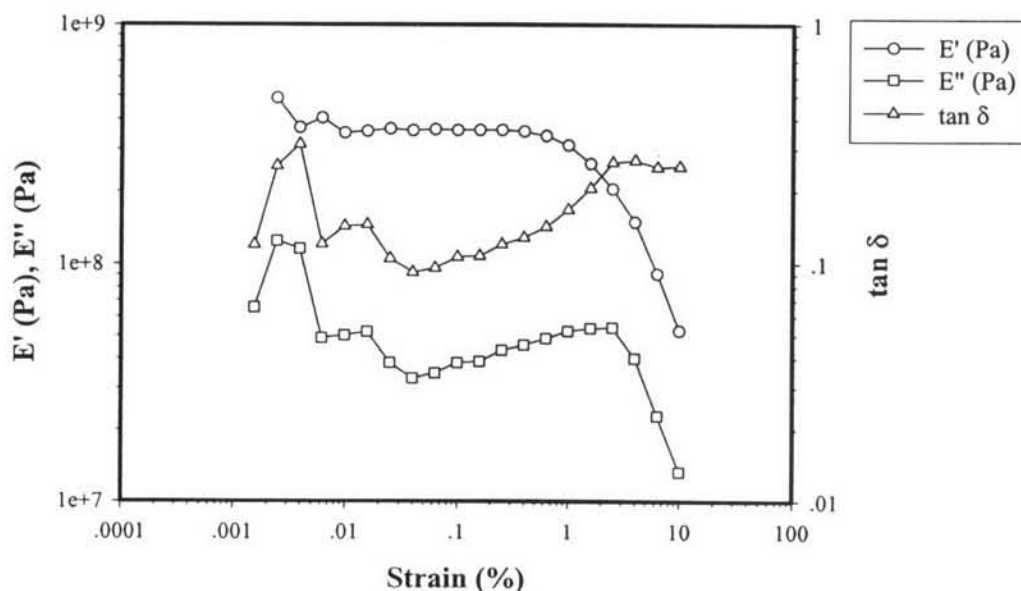
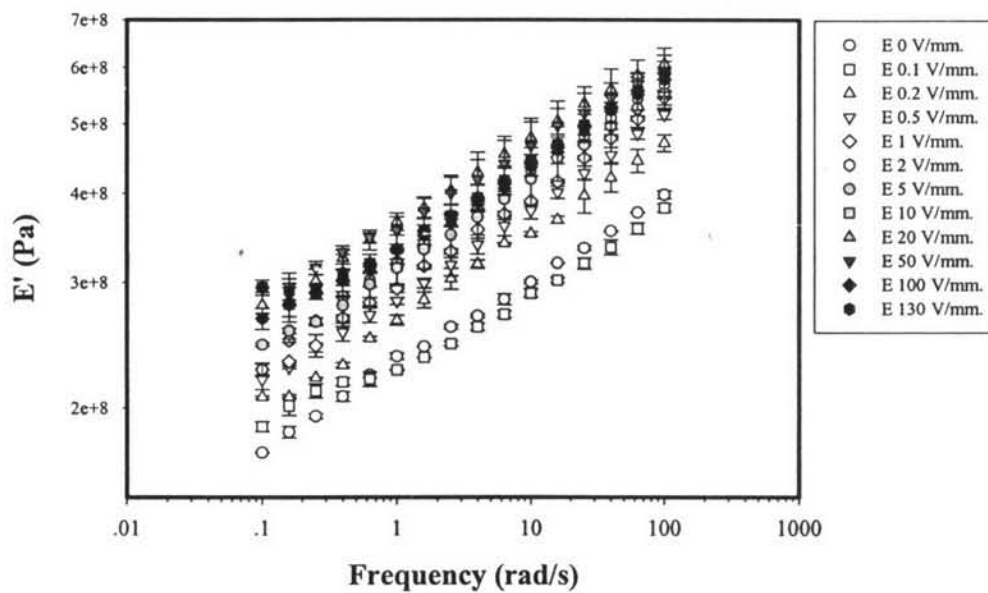
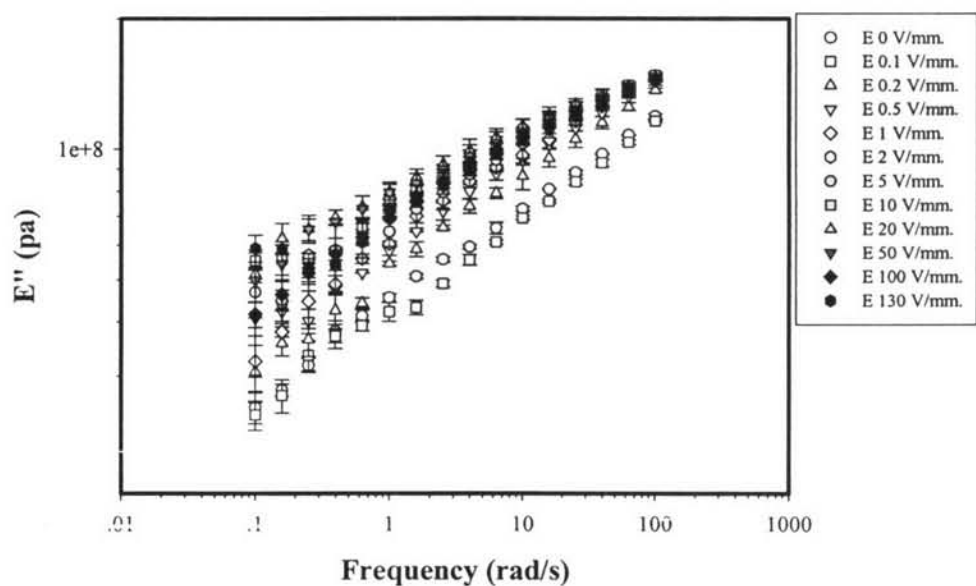


Figure L1 Strain sweep test of pure PVA electrospun fibers at $E = 0$ V/mm (frequency 1.0 rad/s, 27°C).

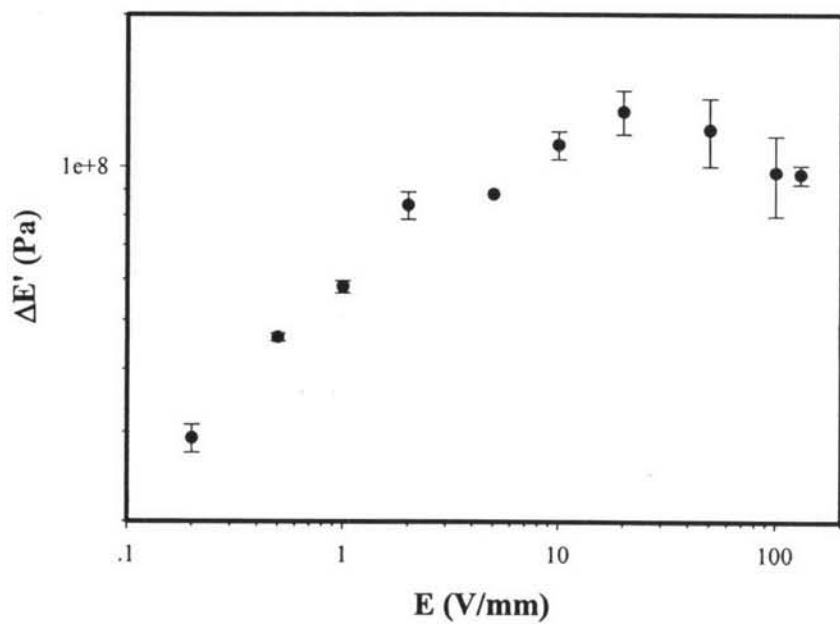


(a)

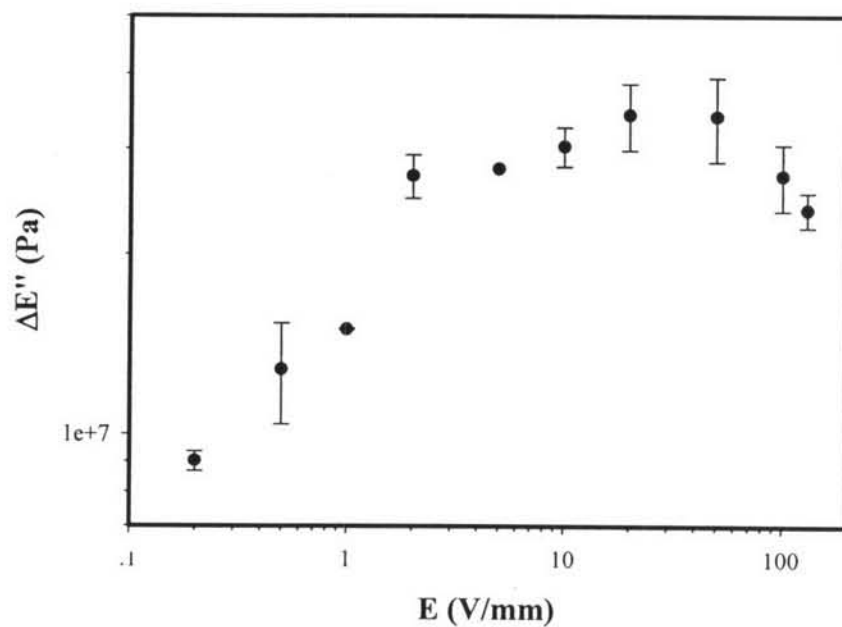


(b)

Figure L2 Frequency sweep test of pure PVA electrospun fibers at various electric field strengths (Strain = 0.3 %, 27°C): (a) = E' and (b) = E'' .



(a)



(b)

Figure L3 Responses of the moduli of pure PVA electrospun fibers vs. electric field strength, frequency = 1.0 rad/s and strain = 0.3 % at 27°C: (a) storage moduli [$\Delta E'(w)$] and (b) loss moduli [$\Delta E''(w)$].

L2. 1 wt% CB-PVA

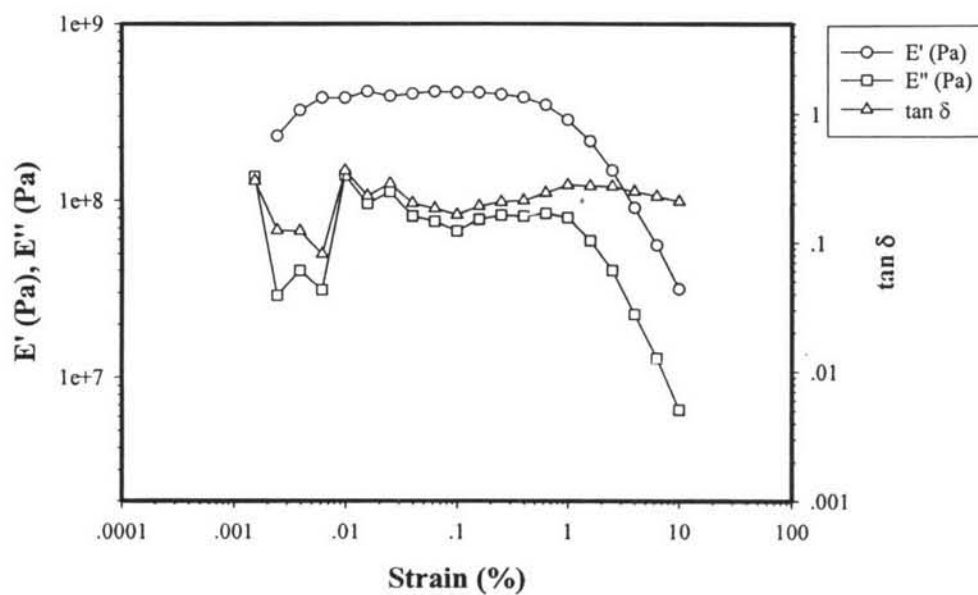
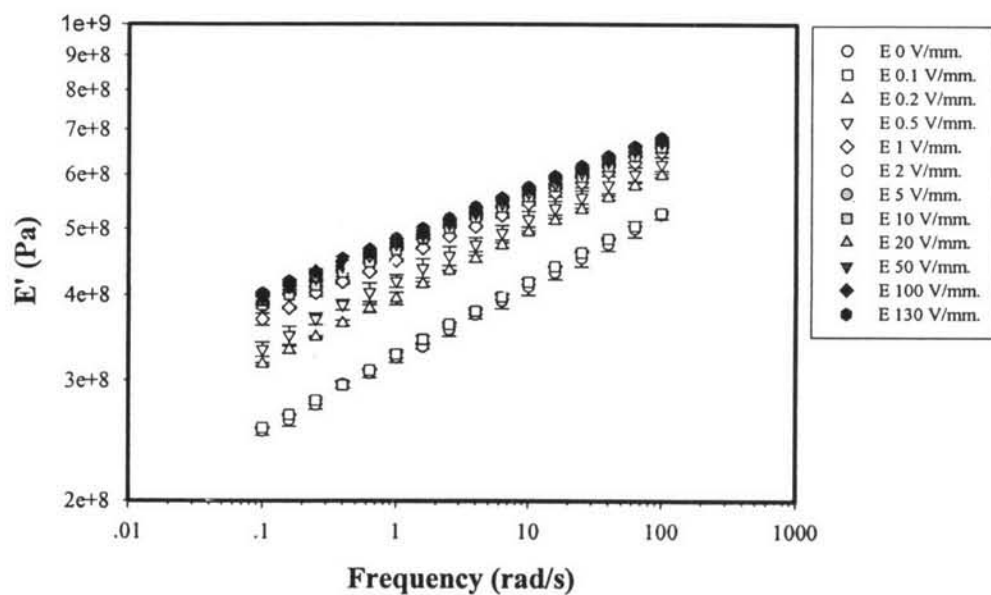
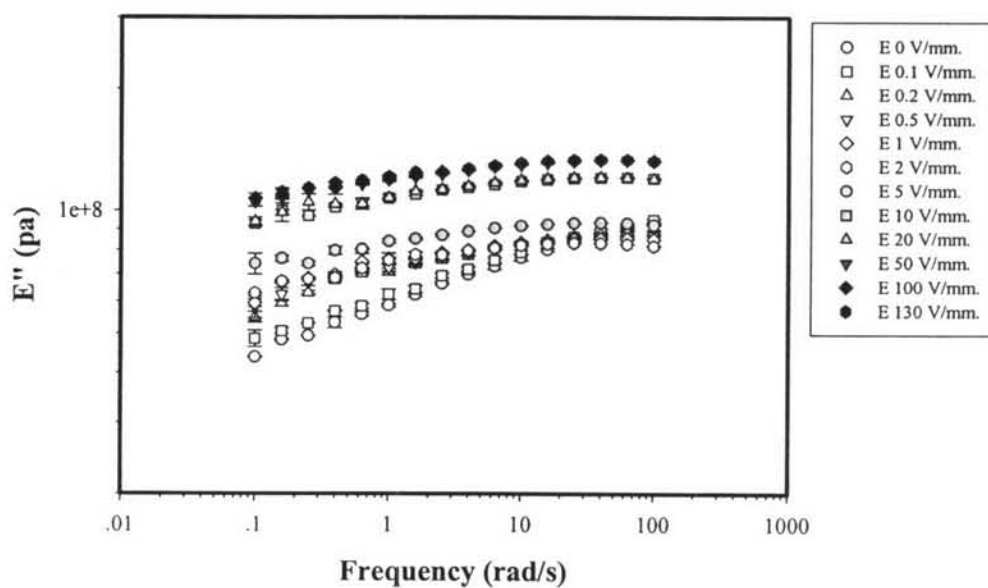


Figure L4 Strain sweep test of 1 wt% CB-PVA electrospun fibers at $E = 0$ V/mm (frequency 1.0 rad/s, 27°C).

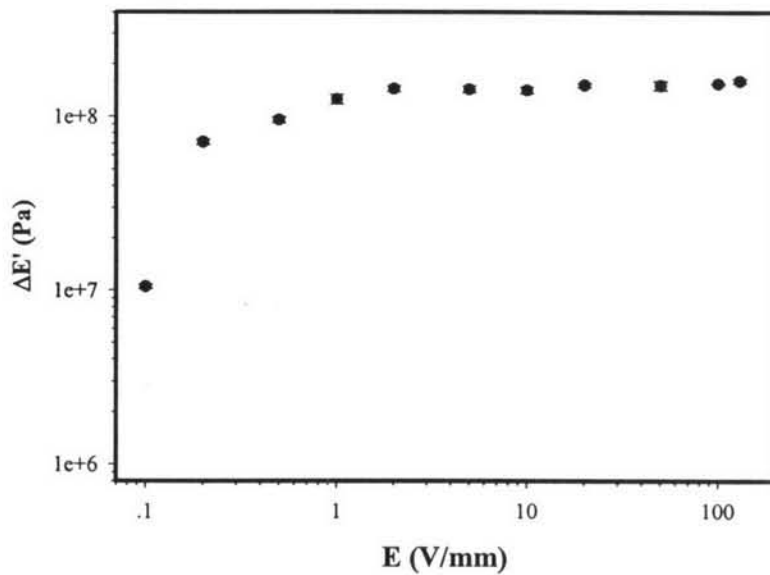


(a)

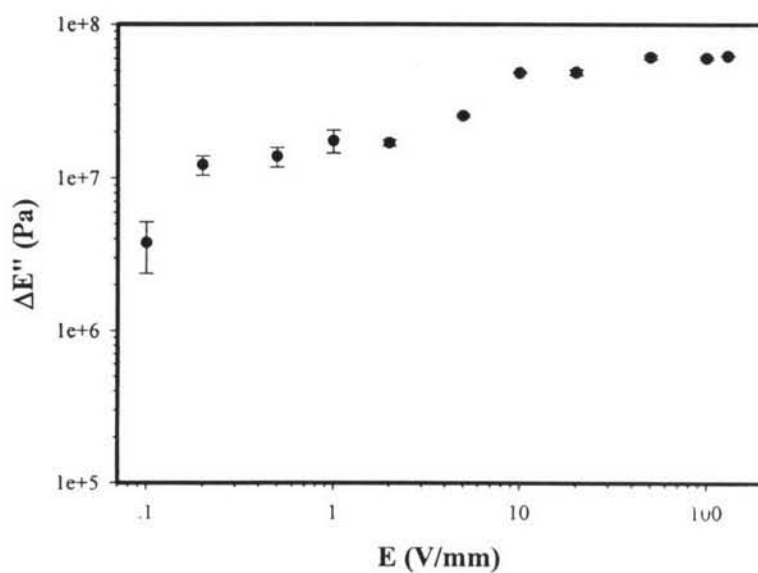


(b)

Figure L5 Frequency sweep test of 1 wt% CB-PVA electrospun at various electric field strengths (Strain = 0.3 %, 27°C): (a) = E' and (b) = E'' .



(a)



(b)

Figure L6 Responses of the moduli of 1 wt% CB-PVA electrospun fibers vs. electric field strength, frequency = 1.0 rad/s and strain = 0.3 % at 27°C: (a) storage moduli [$\Delta E'(w)$] and (b) loss moduli [$\Delta E''(w)$].

L3. 10 wt% CB-PVA

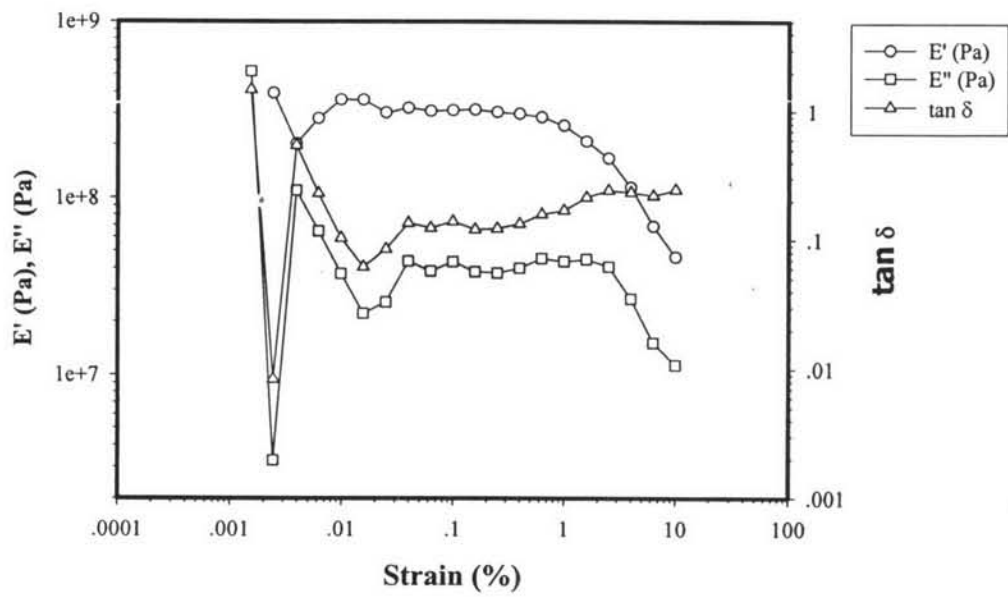
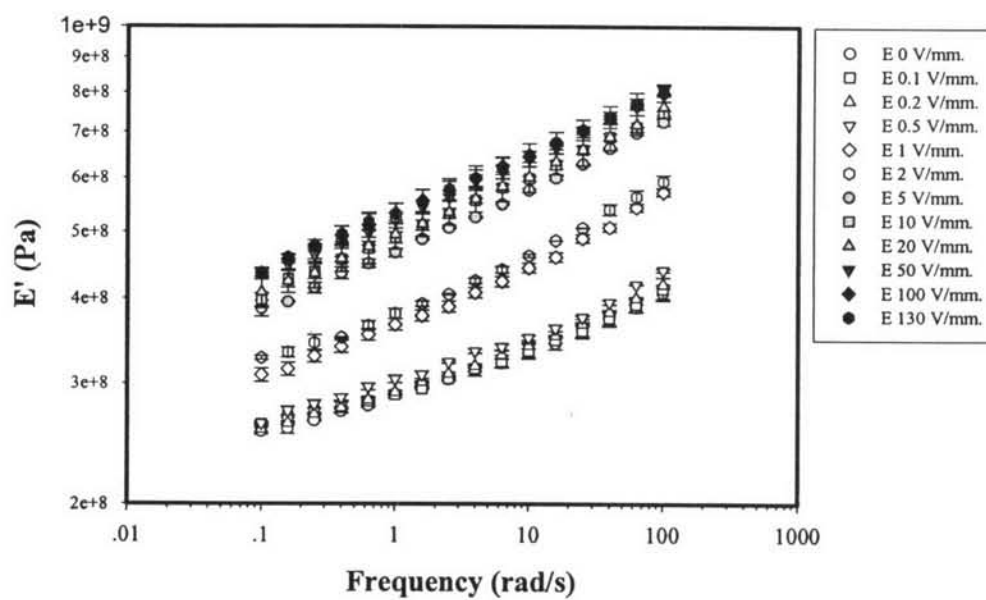
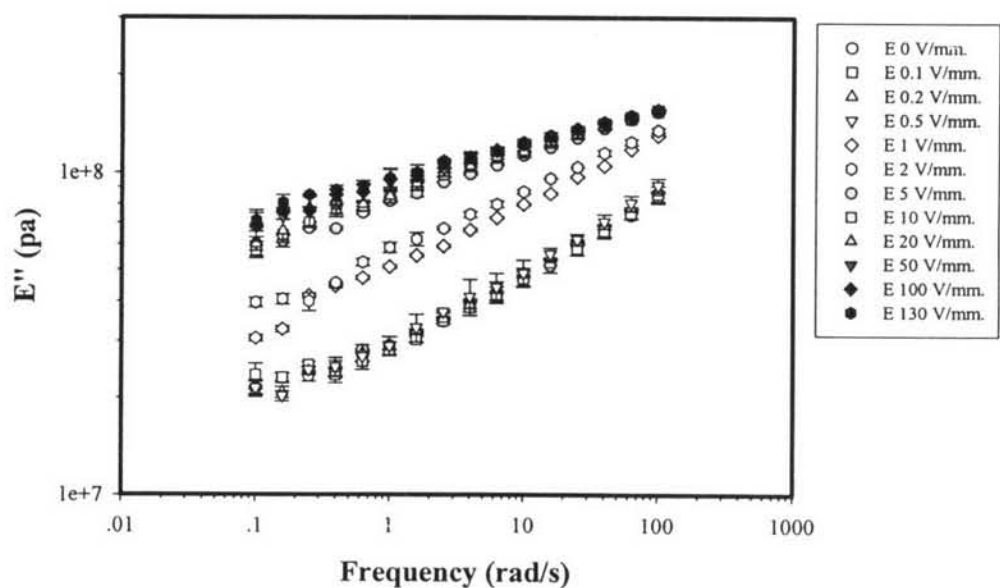


Figure L7 Strain sweep test of 10 wt% CB-PVA electrospun fibers at $E = 0$ V/mm (frequency 1.0 rad/s, 27°C).

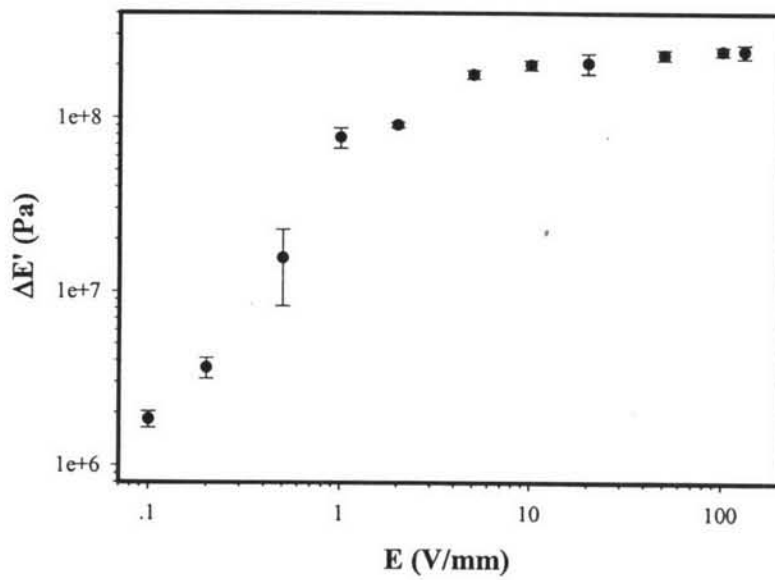


(a)

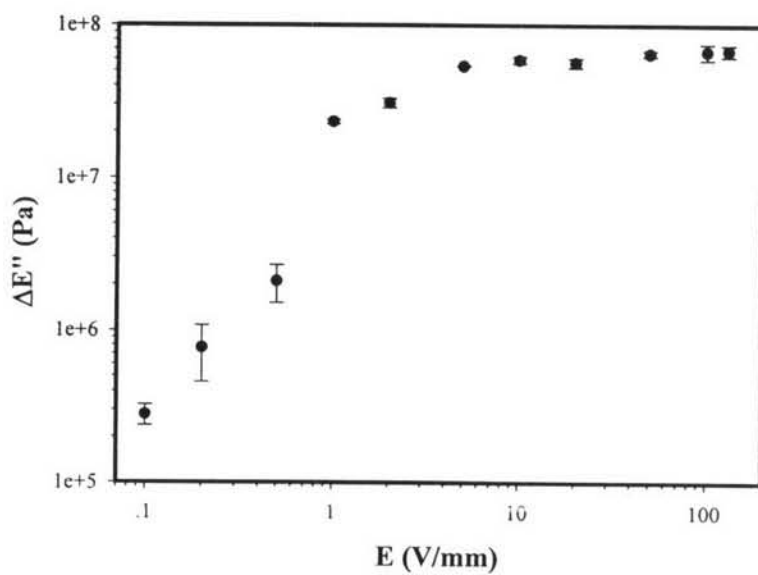


(b)

Figure L8 Frequency sweep test of 10 wt% CB-PVA electrospun fibers at various electric field strengths (Strain = 0.3 %, 27°C): (a) = E' and (b) = E'' .



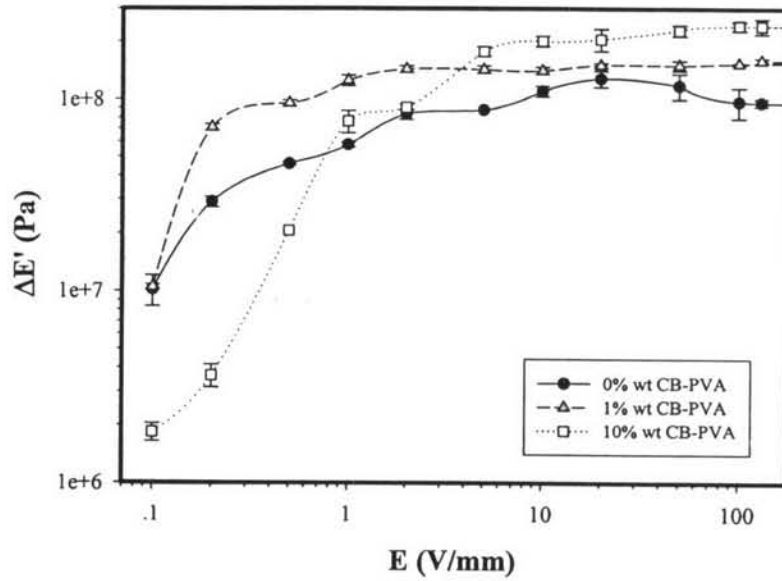
(a)



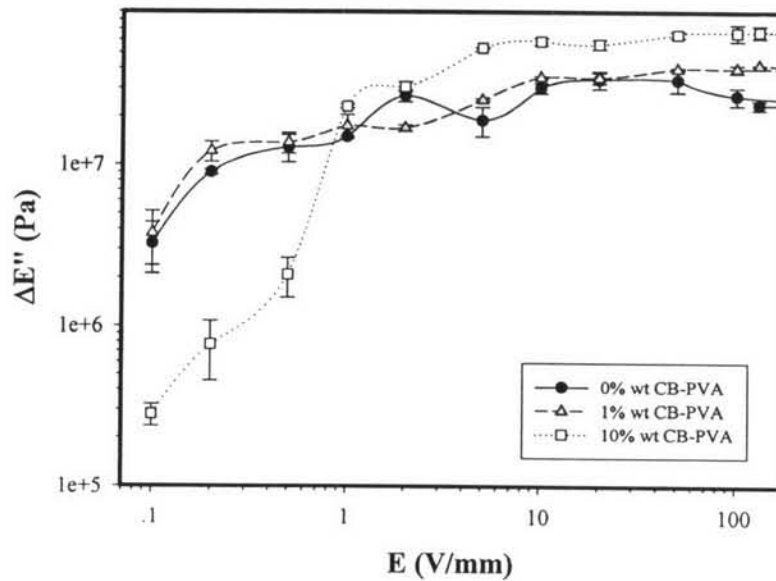
(b)

Figure L9 Responses of the moduli of 10 wt% CB-PVA electrospun fibers vs. electric field strength, frequency = 1.0 rad/s and strain = 0.3 % at 27°C: (a) storage moduli [$\Delta E'(w)$] and (b) loss moduli [$\Delta E''(w)$].

L5. Conclusions of Electrorheological Properties

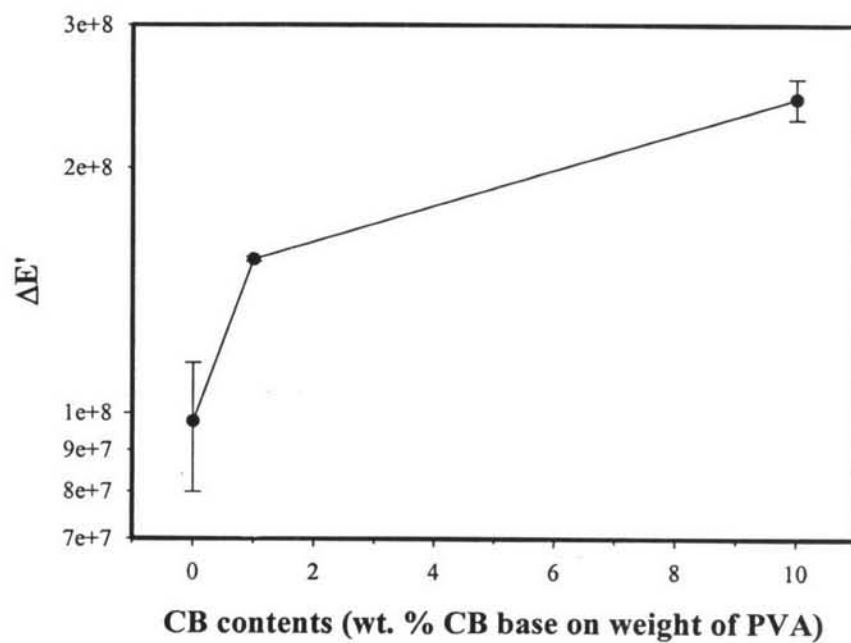


(a)

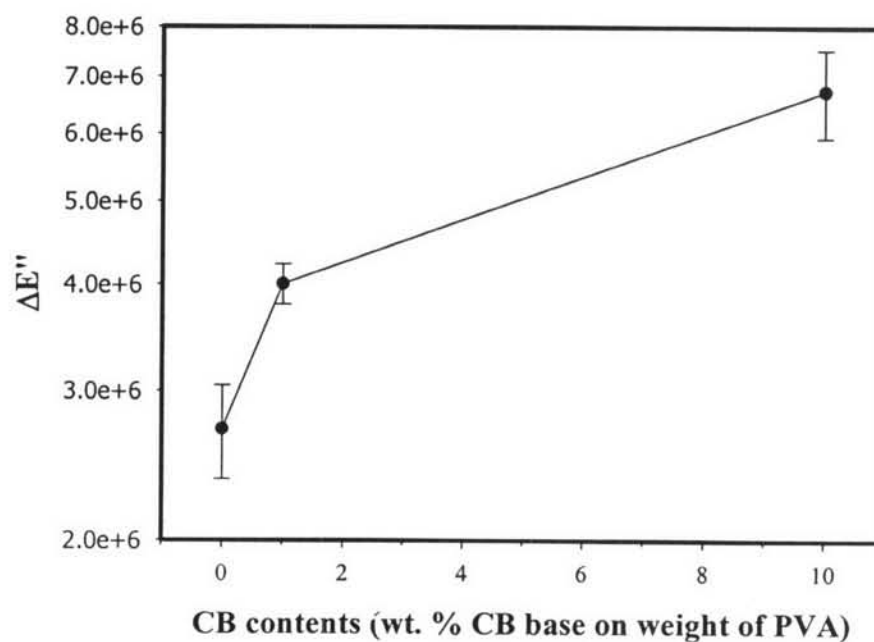


(b)

Figure L10 Responses of the moduli of pure PVA and CB-PVA composite electrospun fibers vs. electric field strength at various compositions of CB, frequency = 1.0 rad/s and Strain = 0.3 % at 27°C: (a) storage moduli [$\Delta E'(w)$] and (b) loss moduli [$\Delta E''(w)$].



(a)



(b)

Figure L11 Effect of carbon black composition on responses of the moduli of carbon black nanoparticle-filled electrospun nanofibers at electric field = 100 V/mm: (a) storage moduli [$\Delta E'(w)$] and (b) loss moduli [$\Delta E''(w)$].

CURRICULUM VITAE

Name: Mr. Surawut Chuangchote

Date of Birth: May 21, 1981

Nationality: Thai

University Education:

2000-2004 Bachelor Degree of Petrochemical and Polymeric Materials, Faculty of Engineering and Industrial Technology, Silpakorn University, Nakhon Pathom, Thailand.

Working Experience:

2003 Position: R&D Trainee

Company name: PI Industry Co.,Ltd. (Innovation Group)

Publications (International Journals):

1. Chuangchote, S. and Supaphol, P. (2006) Fabrication of aligned poly(vinyl alcohol) nanofibers by electrospinning. Journal of Nanoscience and Nanotechnology, 6(1), 125-129.